NASA Technical Paper 1237

Optimal Guidance and Control for Investigating Aircraft Noise-Impact Reduction

Elwood C. Stewart and Thomas M. Carson

MAY 1978

NASA

NASA Technical Paper 1237

Optimal Guidance and Control for Investigating Aircraft Noise-Impact Reduction

Elwood C. Stewart and Thomas M. Carson
Ames Research Center
Moffett Field, California

National Aeronautics
and Space Administration

**Scientific and Technical
Information Office**

1978

TABLE OF CONTENTS

NOTATION

a_o total acceleration, m/sec^2

a_v longitudinal acceleration, m/sec^2

a_γ normal acceleration, m/sec^2

a_ψ lateral acceleration, m/sec^2

C_D drag coefficient

C_L lift coefficient

c_β $d_i - s_i$ (see fig. 2)

D aerodynamic drag, N

d_i ground-track distance between way points

L aerodynamic lift, N

ℓ_i direction cosine of ith ground-track segment, $\begin{pmatrix}\alpha_i \\ \beta_i\end{pmatrix}$

m_i ith ground-track segment length, m

R turn radius in ground track, m

s_i ground-track distance from last way point to next turn (see fig. 2)

T thrust, N

V longitudinal velocity, m/sec

W weight of vehicle, N

X position vector in horizontal plane, $\begin{pmatrix}x_i \\ y_i\end{pmatrix}$, m

x displacement in x direction of local earth-fixed coordinate system, m

y displacement in y direction of local earth-fixed coordinate system, m

Z position vector in vertical plane, $\begin{pmatrix}\sigma_i \\ z_i\end{pmatrix}$, m

z displacement in z direction of local earth-fixed coordinate system, m

Δz change in z as a result of vertical acceleration (see fig. 3)

α angle of attack, deg

γ flight path angle, angle between velocity vector and horizontal plane, deg

Δ distance along the trajectory, m

δ_F flap deflection, deg

η thrust angle, between body axis and thrust vector, deg

Θ change in inclination angle, deg (see fig. 4)

θ_j change in heading of jth curved segment, deg

ρ radius of flight path in vertical plane, m

σ distance along ground track, m

ϕ roll angle, angle about the velocity vector, deg

ψ heading angle, angle between a reference direction in horizontal plane and projections of V in horizontal plane, deg

Note: Italics for the symbol denote quantities defined in a vertical plane and are analogous to those nonitalicized letters in the ground-track plane.

OPTIMAL GUIDANCE AND CONTROL FOR INVESTIGATING AIRCRAFT NOISE-IMPACT REDUCTION

Elwood C. Stewart and Thomas M. Carson

Ames Research Center

SUMMARY

As part of a NASA program to investigate technical approaches for increasing the terminal area effectiveness of advanced short-haul aircraft, this report is concerned with a methodology for investigating the reduction of community noise impact. There are a number of computer programs available for the generation of noise footprints, all of which require various input data that are usually unavailable. This report is concerned with the development of two models to provide such data: a guidance generator and an aircraft control generator suitable for various current and advanced types of aircraft. The guidance generator produces the commanded path information from inputs chosen by an operator from a graphic scope display of a land-use map of the terminal area. The guidance generator also produces smoothing at the junctions of straight-line paths. The aircraft control generator determines the optimal set of the available controls such that the aircraft will follow the commanded path. The solutions for the control functions are given and shown to be dependent on the class of aircraft to be considered, that is, whether the thrust vector is rotatable and whether the thrust vector affects the aerodynamic forces. For the class of aircraft possessing a rotatable thrust vector, the solution is redundant; this redundancy is removed by the additional condition that the noise impact be minimized. Information from both the guidance generator and the aircraft control generator is used by the footprint program to construct the noise footprint.

The complete package of models provides a useful methodology for constructing an interactive graphics tool for rapidly assessing the effects of different aircraft technologies, flight paths, aircraft mixes, and other variables, and for the minimization of noise impact. These effects are illustrated, utilizing an existing footprint program, by several examples which consist of three broad classes of CTOL and V/STOL aircraft.

INTRODUCTION

NASA has been engaged in a program to investigate technical approaches for increasing the terminal area effectiveness of advanced short-haul aircraft. The program is intended to provide guidance to NASA's advanced aircraft technology program. The principal purpose of the program is to investigate the impact of various technical alternatives for increasing the effectiveness of short-haul aircraft in terms of airport airside capacity and delay, community

noise, air pollution, fuel consumption, and ride quality. The technical alternatives include various advanced aircraft, their greater operational bounds and range of flight paths, and avionics.

This report is concerned with the effects of aircraft noise. Because of public concern with environmental issues, the importance of the effects of aircraft noise has increased significantly in recent years. We are concerned here with developing a methodology for examining the trade-offs between technical alternatives and community noise impact.

A key tool in the assessment of noise impact has been the development of noise footprint models and programs. Common to all these models and programs, however, is the need to generate reliable input information so as to render the results more realistic and to enhance their use in examining the many variables and alternatives associated with noise reduction.

The input information is of two distinct types. First, a noise footprint program must be supplied with a description of the aircraft path. For three-dimensional path optimization purposes, the desired aircraft path is best supplied by a guidance generator which utilizes basic information from land-use maps. In this way, the guidance generator generates desired or optimal paths which are directed over areas that are less sensitive to noise. The guidance generator also generates smoothing, that is, smooth commanded paths at the junctions of straight-line segments so as to avoid unrealistically high accelerations.

Second, the noise-footprint program must be supplied with aircraft control function information in order to determine the noise footprint based on stored information in the footprint program. How much of the control information is required depends on the particular footprint program. Most programs inherently assume isotropic noise characteristics, and for them only one of the aircraft controls, the engine parameter (such as engine thrust, throttle setting, etc.) is required. A more sophisticated footprint program that could account for anisotropic noise characteristics would require all the aircraft control functions — the engine parameter, the directional control of the active thrusting forces, bank angle, and angle of attack. In any case, it is necessary to relate the aircraft control functions to the path being flown as specified by the guidance generator. This is best accomplished by utilizing the aircraft equations of motion to derive an aircraft control generator that determines the optimal set of the available controls from which those required by the footprint program are taken.

In this report, we derive the models for generating the input information required by noise footprint models or programs. The two models are a guidance generator and an aircraft control generator suitable for various types of current and advanced aircraft. These two models will be made compatible with a particular noise footprint program, widely used in Government and industry, that was developed several years ago by Serendipity for the Department of Transportation (refs. 1 and 2). The models could be used with a more general footprint program taking into account anisotropic noise since all the required information is available from the models developed here.

The complete package, when implemented, provides a useful interactive graphics optimization tool for rapidly assessing the effects of different aircraft technologies, flight paths, aircraft mixes, and other variables, and for minimizing of noise effects. Several examples are given to illustrate applications of the methodology to broad categories of advanced aircraft.

GENERAL STRUCTURE

The general structure of a system incorporating a noise footprint model, the guidance generator, and the aircraft-control system model are shown in sketch (a).

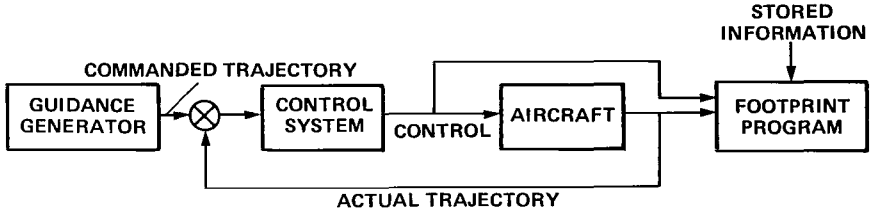

Sketch (a)

The guidance generator produces the desired trajectory and the control system then attempts to make the aircraft follow that trajectory. The final element is the footprint program which requires three kinds of information: (1) stored information describing the noise characteristics of the aircraft; for the footprint program used here this stored information consists of the noise characteristics expressed as a function of the slant range and the engine noise parameter; (2) input information describing the aircraft trajectory; and (3) input information defining the variation of the aircraft controls during the flight; for the footprint program to be used here, only the engine parameter is utilized.

It will be desirable to modify the structure from that just discussed to accommodate the requirements of the particular noise footprint program to be used, and to achieve certain simplifications. In this regard, there are three considerations.

First, the footprint program requires the trajectory to be parameterized in terms of segment lengths, parts of circles, and inclination angles. Second, since the aircraft can follow the commanded trajectory exactly (in the absence of control errors), the system structure shown above can be simplified as shown in sketch (b) on the following page.

Third, as a result of the modified structure, it is necessary to generate the optimal aircraft controls based on the desired trajectory, as indicated in the sketch by the aircraft control generator. The situation shown is for the footprint program to be used here in which only one of the controls, the engine parameter T is used. For a more general program, all the controls

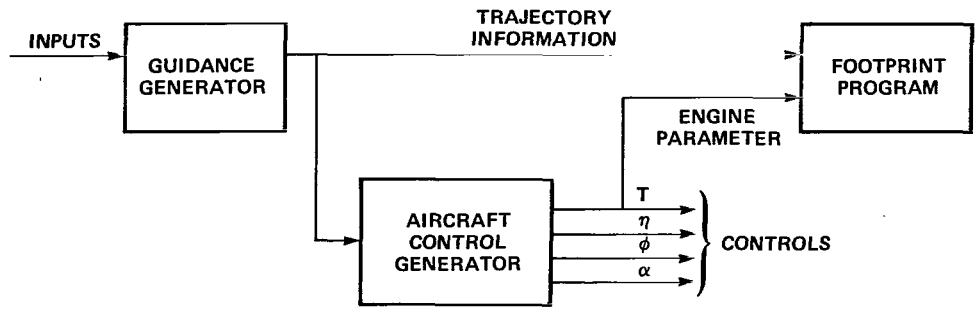

Sketch (b)

are available for use. As will be seen later, the additional controls consist of the directional control of the active thrusting forces η, bank angle ϕ, and angle of attack α. This information, in conjunction with the trajectory information, provides all the information that would be required by any footprint program.

GUIDANCE GENERATOR

Introduction

The purpose of the guidance generator is to generate information about the desired path of the aircraft. In this section we will consider how to generate this information from available data and how to generate it in a form that will be compatible with the existing footprint program.

First, consider the input information available to the guidance generator. The determination of the desired or optimal ground track information for the purpose of minimizing noise effects must necessarily start with land-use maps of the airport and the surrounding community. This will permit the selection of candidate flight paths that are directed away from noise-sensitive areas. The most convenient way in which to display such maps is on a graphic scope display since this achieves good man-machine interaction for the noise minimization process. In this form, the graphics display readily incorporates provision for the experimenter to specify certain trial way-points that are the start and end points of straight-line segments of the ground track. The coordinates of these way-points are readily stored by the computer and hence are available as inputs to the guidance generator. To completely define the path of the aircraft it is also necessary to specify the velocity and inclination angle along each segment. And finally, it will be necessary to specify the tolerable acceleration levels to enable the generation of suitably smoothed transitions between straight-line segments, as will be discussed shortly.

Next, consider the form of the output of the guidance generator. Since the guidance generator output will be used directly by the existing footprint program which is to be left unchanged, this output must be of a form suitable

for the footprint program. The latter requires that the flight path be described by a sequence of segments in which each segment is defined by the following four variables:

m_k or θ_k kth segment length in horizontal plane, m, or kth subtended turn angle, deg

γ_k inclination angle, climb or descent, for kth segment, deg

T_k engine noise parameter for the kth segment, percent of maximum

R_k turn radius of kth segment, m
0 = straight
+ = clockwise
- = counterclockwise

The parameters, m_k, θ_k, and R_k, need to be provided by the guidance generator, the γ_k is specified as an input, and the T_k is to be determined by the aircraft control generator.

An important consideration in the generation of the commanded trajectory is the need to generate a smooth transition between straight-line segments so as to avoid unrealistic situations at the junction of straight-line segments. This will be done in the general three-dimensional case.

The transition between straight-line segments is characterized by various combinations of lateral, normal, and longitudinal accelerations. There are seven possible combinations of motion on the transition segments as enumerated by the following:

Case	$\dot{V}$	$\dot{\gamma}$	$\dot{\psi}$
1	0	$\neq 0$	$\neq 0$
2	0	0	$\neq 0$
3	0	$\neq 0$	0
4	$\neq 0$	0	0
5	$\neq 0$	0	$\neq 0$
6	$\neq 0$	$\neq 0$	0
7	$\neq 0$	$\neq 0$	$\neq 0$

For each of these cases, it will be necessary to generate the information required by the footprint program. However, many of the cases are similar and the results for some may be constructed by combining other cases, as will be seen in later developments. Basically, there are three types of transition trajectories which need to be considered:

Type A: arcs with free end points
Type B: arcs with constrained end points
Type C: longitudinal acceleration with fixed end points

Rather than discuss each of these types in general and then apply them to each of the seven possible cases, it will be more meaningful to discuss them in the

context of the appropriate case. In particular, the correspondence will be as follows:

Type trajectory	Case
A	1 (lateral equations)
B	1 (normal equations)
C	4

The remainder of the seven possible cases can be constructed from the results for these basic trajectory types.

To clarify the interrelation of the various cases, a flow graph of the computations to be discussed in the following sections is shown in figure 1. The rectangles contain the variables that are to be computed according to the appropriate equations to follow. The indicated tests are made to determine whether ψ, γ, and V are required to change. Each possibility, representing one of the seven cases, leads to a different path on the flow graph. Dotted lines indicate a flow of information in both directions between rectangles in a manner made clear by the appropriate equations. The output of the guidance generator is indicated by the seven possible outputs and by a list of the output variables.

Case 1. Lateral and Normal Accelerations

In this section the development of the equations necessary to generate the required outputs from the available inputs will be considered. The general case, in which the aircraft is turning and the inclination angle is changing, will be considered here, and special cases will be dealt with later. Reference should be made to figure 1 for the flow graph clarifying the computations to be discussed.

Lateral equations (Type A trajectory: arc with free end points)- Let the points which are selected on the graphic map display of the horizontal plane be numbered by $X_0, X_1, \ldots X_k \ldots X_n$ where

$$X_k = \begin{bmatrix} x_k \\ y_k \end{bmatrix} \tag{1}$$

and the components x_k and y_k represent the coordinates of the ground-track display. Figure 2 illustrates the general situation of the three-dimensional trajectory which is based on the three chosen points X_α, X_β, and X_γ. The ith and kth segments are straight-line segments and the jth segment is a circular segment which forms the smooth transition between the ith and kth segments.

Now consider how the quantities m_i and m_k, required for the footprint program, can be determined from the three general points shown in figure 2. In general, the two points X_α and X_β, connected by the ith line, will be

separated by a distance d_i and the line connecting these two points will have a direction cosine ℓ_i given by

$$d_i^2 = (X_\beta - X_\alpha)^T(X_\beta - X_\alpha) \tag{2}$$

$$\ell_i = \frac{X_\beta - X_\alpha}{d_i} \equiv \begin{pmatrix} \alpha_i \\ \beta_i \end{pmatrix} \tag{3}$$

Furthermore, any point X on the ith line connecting X_α and X_β is given by

$$X = X_\alpha + s\ell_i \tag{4}$$

where s is the distance between X_α and X. In particular, for the tangency points X_p and X_q shown in figure 2, we have

$$X_p = X_\alpha + s_i\ell_i = X_\beta - (d_i - s_i)\ell_i \tag{5}$$

$$X_q = X_\beta + c_\beta\ell_k \tag{6}$$

The center of the circular arc X_c is given in terms of X_p and X_q by a relation similar to equation (4):

$$X_c = X_p + R\ell_p \tag{7}$$

$$X_c = X_q + R\ell_q \tag{8}$$

where R is the radius of the circular arc and ℓ_p and ℓ_q are the direction cosines of the radii between X_p and X_c, and X_q and X_c, respectively. The determination of these three quantities is deferred temporarily. Now, by equating (7) and (8) and substituting for X_p and X_q from equations (5) and (6) we obtain

$$A\begin{pmatrix} s_i \\ c_\beta \end{pmatrix} = D \tag{9}$$

where

$$\left.\begin{aligned} A &= (\ell_i - \ell_k) \\ D &= d_i\ell_i + R(\ell_q - \ell_p) \end{aligned}\right\} \tag{10}$$

The solution is

$$\begin{pmatrix} s_i \\ c_\beta \end{pmatrix} = A^{-1}D \tag{11}$$

and these are the quantities necessary to determine the segments required for the footprint program. That is, the ith and kth straight-line segments shown in figure 2 are

$$m_i = s_i - c_\alpha \tag{12}$$

$$m_k = s_k - c_\beta \tag{13}$$

The sequence of calculations in equations (11)-(13) needs some clarification. At the start, when the aircraft is taking off, $c_\alpha = 0$, so that s_i from equation (11) is all that is needed in equation (12) to determine m_i. For the next segment, m_k in equation (13), the s_k comes from a second application of equation (11) using three new points starting with X_β while the c_β is known from the first application of equation (11). In similar fashion the process continues. On the last segment, we must have $s_k = d_k$ so that

$$m_k = d_k - c_\beta \quad \text{(last segment)} \tag{14}$$

As for the jth segment, both the subtended angle θ_j and the radius R are required for the footprint program and for the preceding equation (11). The subtended angle is given by the fundamental relation

$$\cos \theta_j = \ell_p{}^T \ell_q \tag{15}$$

The footprint program does not recognize a sign on this angle so that the input to the footprint program is

$$\theta_j = \left|\cos^{-1} \ell_p{}^T \ell_q\right| \tag{16}$$

The sign information is accounted for by specifying R as >0 or <0 depending on whether θ_j was clockwise or counterclockwise. The manner in which this is done will be discussed shortly.

The magnitude of the radius must be determined by the acceleration to be allowed. The component of the velocity in the ground-track horizontal plane for the jth segment is $V_j \cos \gamma_j$. Hence, the lateral acceleration a_ψ is given by

$$a_\psi = V_j \dot{\psi} \cos \gamma_j = \frac{(V_j \cos \gamma_j)^2}{R} \tag{17}$$

R should be based on the total acceleration, rather than determined from this equation; for this reason the determination of R is deferred temporarily.

It still remains to determine the equations for ℓ_p and ℓ_q. It would appear that because of the perpendicularity of the radius and the ith and kth segments, the conditions

$$\ell_i^T \ell_p = 0 \tag{18}$$

$$\ell_k^T \ell_q = 0 \tag{19}$$

would be sufficient to define ℓ_p and ℓ_q. However, this is not the case. In the approach to be used here, use will be made of sketch (c).

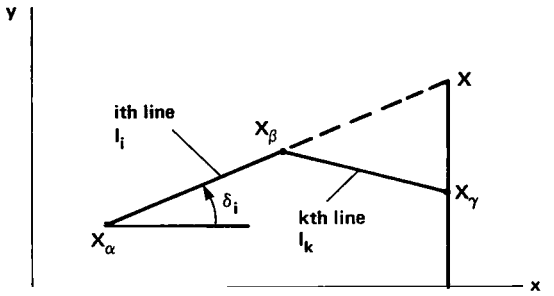

Sketch (c)

We will determine whether the extension of line i lies to the left or right of line k. Let the line i be extended beyond point X_β. Any point on this extension a distance s from X_α is given by

$$X = X_\alpha + s\ell_i \tag{20}$$

or

$$\begin{pmatrix} x \\ y \end{pmatrix} = \begin{pmatrix} x_\alpha \\ y_\alpha \end{pmatrix} + s\begin{pmatrix} \alpha_i \\ \beta_i \end{pmatrix} \tag{21}$$

Letting $x = x_\gamma$, we have

$$\begin{pmatrix} x_\gamma \\ y \end{pmatrix} = \begin{pmatrix} x_\alpha \\ y_\alpha \end{pmatrix} + s\begin{pmatrix} \alpha_i \\ \beta_i \end{pmatrix}$$

The only unknowns here are y and s and the solution for y is

$$y = y_\alpha + \frac{x_\gamma - x_\alpha}{\alpha_i}\beta_i$$

Now it is clear from the geometry of the situation, recalling from equation (3) that $\alpha_i \equiv \cos\delta_i$ (see sketch (c)), that

$$\alpha_i > 0 \quad \text{and} \quad \begin{cases} y_\gamma > y \Rightarrow \text{left turn} \\ y_\gamma < y \Rightarrow \text{right turn} \end{cases}$$

$$\alpha_i < 0 \quad \text{and} \quad \begin{cases} y_\gamma < y \Rightarrow \text{left turn} \\ y_\gamma > y \Rightarrow \text{right turn} \end{cases}$$

A left turn implies that R lies on the left of segment i while a right turn implies that R lies on the right of segment i. Define the components of ℓ_p and ℓ_q by

$$\ell_p \equiv \begin{pmatrix} \alpha_p \\ \beta_p \end{pmatrix} \qquad \ell_q \equiv \begin{pmatrix} \alpha_q \\ \beta_q \end{pmatrix}$$

Now for a left turn we have

$$\alpha_p = \cos\left(\delta_i + \frac{\pi}{2}\right) = -\sin\,\delta_i = -\beta_i$$

$$\beta_p = \sin\left(\delta_i + \frac{\pi}{2}\right) = \cos\,\delta_i = \alpha_i$$

In a similar way, the components of ℓ_q are related to the segment k. Thus, we have

$$\text{left turn} \Rightarrow \begin{cases} \ell_p = \begin{pmatrix} -\beta_i \\ \alpha_i \end{pmatrix} \\ \ell_q = \begin{pmatrix} -\beta_k \\ \alpha_k \end{pmatrix} \end{cases}$$

For a right turn, the relations for ℓ_p are

$$\alpha_p = \cos\left(\delta_i - \frac{\pi}{2}\right) = \sin\,\delta_i = \beta_i$$

$$\beta_p = \sin\left(\delta_i - \frac{\pi}{2}\right) = -\cos\,\delta_i = -\alpha_i$$

The components of ℓ_q are related in similar fashion to the segment k. Thus

$$\text{right turn} \Rightarrow \begin{cases} \ell_p = \begin{pmatrix} \beta_i \\ -\alpha_i \end{pmatrix} \\ \ell_q = \begin{pmatrix} \beta_k \\ -\alpha_k \end{pmatrix} \end{cases}$$

The preceding results are condensed by the following:

$$\ell_p \equiv \begin{pmatrix} \alpha_p \\ \beta_p \end{pmatrix} = \left\{ \operatorname{sgn}[\alpha_i (y - y_\gamma)] \right\} \begin{pmatrix} \beta_i \\ -\alpha_i \end{pmatrix} \tag{22}$$

$$\ell_q \equiv \begin{pmatrix} \alpha_q \\ \beta_q \end{pmatrix} = \left\{ \operatorname{sgn}[\alpha_i (y - y_\gamma)] \right\} \begin{pmatrix} \beta_k \\ -\alpha_k \end{pmatrix} \tag{23}$$

The orthogonality requirements of equations (18) and (19) are evident.

Normal equations (Type B trajectory: arc with constrained end points)- Consider now the motion and normal acceleration required to change the inclination angle. For this purpose the new diagram shown in figure 3 will be convenient. Here the attitude is depicted as a function of the distance σ traversed in the ground track, and the point corresponding to X_α in figure 2 is defined by

$$Z_\alpha \equiv \begin{pmatrix} \sigma_\alpha \\ z_\alpha \end{pmatrix} \tag{24}$$

to reflect the correspondence. Three such points are shown in figure 3. If the normal acceleration occurs between the same points X_p and X_q as for the lateral acceleration, it is clear that the transition trajectory due to normal acceleration is one with fixed end points. Thus, this situation is an example of a type B trajectory with constrained end points.

First, let us determine the transition trajectory between the segments. The ith segment has the direction cosine ℓ_i given by

$$\ell_i \equiv \begin{pmatrix} \zeta_i \\ \eta_i \end{pmatrix} = \begin{pmatrix} \cos \gamma_i \\ \sin \gamma_i \end{pmatrix} \tag{25}$$

where the γ_i value is known, that is, specified; similarly for ℓ_k. It is important to note here that in the equations to follow, γ is taken to be positive for angles above the horizontal and negative below. Thus, the range of interest is $-\pi/2 < \gamma < \pi/2$. The point Z_p is given by inspection of figure 3 as

$$Z_p = \begin{pmatrix} \sigma_p \\ z_p \end{pmatrix} = \begin{pmatrix} \sigma_\alpha + s_i \\ z_\alpha + s_i \tan \gamma_i \end{pmatrix} \tag{26}$$

$$Z_q = \begin{pmatrix} \sigma_q \\ z_q \end{pmatrix} = \begin{pmatrix} \sigma_\alpha + s_i + R\theta_j \\ z_\alpha + s_i \tan \gamma_i + \Delta z \end{pmatrix} \tag{27}$$

where Δz is the increase in z along segment j. The curvature required in the transition can be found by locating the center Z_c of the circular arc as follows:

$$Z_c = Z_p + \ell_p \rho \tag{28}$$

$$Z_c = Z_q + \ell_q \rho \tag{29}$$

where ℓ_p and ℓ_q are the direction cosines of the radii shown in figure 3, and are represented by

$$\ell_p = \begin{pmatrix} \zeta_p \\ \eta_p \end{pmatrix} \tag{30}$$

$$\ell_q = \begin{pmatrix} \zeta_q \\ \eta_q \end{pmatrix} \tag{31}$$

The determination of the direction cosines will be deferred temporarily. Equating equations (28) and (29) and utilizing equations (26) and (27) we obtain

$$\begin{pmatrix} \sigma_\alpha + s_i \\ z_\alpha + s_i \tan \gamma_i \end{pmatrix} + \rho \begin{pmatrix} \zeta_p \\ \eta_p \end{pmatrix} = \begin{pmatrix} \sigma_\alpha + s_i + R\theta_j \\ z_\alpha + s_i \tan \gamma_i + \Delta z \end{pmatrix} + \rho \begin{pmatrix} \zeta_q \\ \eta_q \end{pmatrix}$$

The solution for the unknowns ρ and Δz is

$$\rho = \frac{R\theta_j}{\zeta_p - \zeta_q} \tag{32}$$

$$\Delta z = \rho(\eta_p - \eta_q) = R\theta_j \frac{\eta_p - \eta_q}{\zeta_p - \zeta_q} \tag{33}$$

and these will be used in the following. It is of interest to note that in the limit as $\gamma_k \to \gamma_i$, $\Delta z = R\theta_j \tan \gamma_i$, and by inspection of figure 3, this can be seen to be the correct limiting value.

The radius ρ just determined can now be used to determine the normal acceleration on the jth segment:

$$a_\gamma = \frac{V_j^2}{\rho} = \frac{V_j^2(\zeta_p - \zeta_q)}{R\theta_j} \tag{34}$$

where equation (32) has been utilized to eliminate ρ. This equation will be used in the next section to determine the lateral turn radius.

The value of Δz determined by equation (33) is used to establish a value for the inclination angle during the transition between straight-line segments. This matter warrants further discussion. When the inclination angles on consecutive straight-line segments are different, that is, $\gamma_i \neq \gamma_k$, the inclination angle γ_j on the circular connecting segment will vary in a continuous manner between γ_i and γ_k. However, the noise footprint program only accepts constant γ values. Consequently, in order to meet this requirement of the footprint program, it is necessary to determine an appropriate constant value for γ_j. This should be done so that the end point Z_q is the same value that would be obtained from the circular segment. Thus,

$$\tan \gamma_j = \frac{\Delta z}{R\theta_j} = \frac{\eta_p - \eta_q}{\zeta_p - \zeta_q} \tag{35}$$

where equation (33) has been used to obtain the expression on the right side.

It is still necessary to determine the direction cosines ℓ_p and ℓ_q, which have been tacitly assumed to be known in the preceeding development. Since ρ in figure 3 is perpendicular to both the ith and kth segment, we have

$$\ell_i^T \ell_p = 0 \tag{36}$$

$$\ell_k^T \ell_q = 0 \tag{37}$$

Using equation (25) in the above equations yields

$$\ell_p \equiv \begin{pmatrix} \zeta_p \\ \eta_p \end{pmatrix} = \begin{pmatrix} \pm\eta_i \\ \mp\zeta_i \end{pmatrix} \tag{38}$$

$$\ell_q \equiv \begin{pmatrix} \zeta_q \\ \eta_q \end{pmatrix} = \begin{pmatrix} \pm\eta_k \\ \mp\zeta_k \end{pmatrix} \tag{39}$$

The orthogonality relation is not sufficient to determine the signs, and more information is needed.

Consider now the determination of the signs of the direction cosines ℓ_p and ℓ_q. From geometric considerations in figure 3 and the way in which γ is defined, it is clear that

$\gamma_i > \gamma_k \Rightarrow \rho$ lies below the path

$\gamma_i < \gamma_k \Rightarrow \rho$ lies above the path

as the aircraft proceeds along the trajectory. Thus for $\gamma_i > \gamma_k$,

$$\zeta_p = \cos\left(\gamma_i - \frac{\pi}{2}\right) = \sin \gamma_i = \eta_i$$

$$\eta_p = \sin\left(\gamma_i - \frac{\pi}{2}\right) = -\cos \gamma_i = -\zeta_i$$

In similar fashion,

$$\zeta_q = \cos\left(\gamma_k - \frac{\pi}{2}\right) = \sin \gamma_k = \eta_k$$

$$\eta_q = -\zeta_k$$

For the other case in which $\gamma_i < \gamma_k$, the components of ℓ_p are

$$\zeta_p = \cos\left(\gamma_i + \frac{\pi}{2}\right) = -\sin \gamma_i = -\eta_i$$

$$\eta_p = \zeta_i$$

and the components of ℓ_q are

$$\zeta_q = -\eta_k$$

$$\eta_q = \zeta_k$$

The equations in this paragraph are valid for $-\pi/2 < \gamma < \pi/2$. The range of γ is restricted because for large angles near 2π the above sequence of equations breaks down, and because $[-\pi/2, \pi/2]$ is the range of practical interest.

The foregoing can be summarized by the following

$$\ell_p \equiv \begin{pmatrix} \zeta_p \\ \eta_p \end{pmatrix} = [\mathrm{sgn}(\gamma_i - \gamma_k)] \begin{pmatrix} \eta_i \\ -\zeta_i \end{pmatrix} \tag{40}$$

$$\ell_q \equiv \begin{pmatrix} \zeta_q \\ \eta_q \end{pmatrix} = [\mathrm{sgn}(\gamma_i - \gamma_k)] \begin{pmatrix} \eta_k \\ -\zeta_k \end{pmatrix} \tag{41}$$

where $-\pi/2 < \gamma < \pi/2$. The orthogonality requirements of equations (36) and (37) are clearly satisfied.

Lateral turn radius- The determination of the lateral turn radius R has been deferred until now so that it could be based on the total acceleration. The total acceleration a_o is given by combining equations (17) and (34):

$$a_o^2 = a_\psi^2 + a_\gamma^2$$

$$= \left[\frac{(V \cos \gamma_j)^2}{R}\right]^2 + \left[\frac{V^2(\zeta_p - \zeta_q)}{R\theta_j}\right]^2 \tag{42}$$

where the j subscript has been suppressed because the velocity is constant on segments i, j, and k. Equation (42) can be solved for R for a specified value of a_o, and the result is

$$R^2 = \frac{1}{a_o^2}\left[(V \cos \gamma_j)^4 + \frac{V^4(\zeta_p - \zeta_q)^2}{\theta_j^2}\right] \tag{43}$$

Since γ_j varies from γ_i to γ_k corresponding to the ends of the jth segment, the maximum acceleration will occur at either end, and a maximum operation is required as shown in equation (45) below. Further, the footprint program requires a sign convention on R to indicate clockwise or counterclockwise turning. The correct sign is obtained from the following:

$$\left.\begin{aligned} &\text{sgn}(\alpha_i)(y - y_\gamma) > 0 \Rightarrow \text{clockwise} \Rightarrow R > 0 \\ &\text{sgn}(\alpha_i)(y - y_\gamma) < 0 \Rightarrow \text{counterclockwise} \Rightarrow R < 0 \end{aligned}\right\} \tag{44}$$

as can be seen from equation (22) and the discussion leading up to it. Thus,

$$R = \text{sgn}[(\alpha_i)(y - y_\gamma)] \max_{n=i,k} \frac{1}{a_o}\left[(V \cos \gamma_n)^4 + \frac{V^4(\zeta_p - \zeta_q)^2}{\theta_j^2}\right]^{1/2} \tag{45}$$

This result determines the lateral turn radius such that the total acceleration will not exceed a specified value. This result is also needed to complete the determination of the normal equations which have been dependent on R.

Case 2. Lateral Acceleration Only

This is a trivial special case of Case 1, and the equations given there are sufficient. In Case 2, there is no change in the inclination angle between consecutive segments, and this includes spiral type motion. The flow graph of the computations involved here are shown in figure 1.

Case 3. Normal Acceleration Only

The guidance equations for the case in which only normal acceleration is required on the transition between straight-line segments are considered here. This includes the planar so-called "two-segment" paths. The trajectory involved is Type A, that is, an arc with free end points. For this reason,

the results for this case are not obtainable from the normal equations for Case 1 since the normal equations there were for a Type-B trajectory, an arc with fixed end points. That is, the junction points of the transition segment for Case 1 were determined by the lateral motion and the normal motion was "fit" to these junction points. In the present case the lateral motion is absent so that the junction points for the normal equations are free. Since the present case is a Type-A trajectory, it is basically the same as for the lateral equations of Case 1, and the results there are immediately applicable. However, there are minor differences, and in order to avoid confusion, the equations and diagram of the situation will be given. Reference should be made to figure 1 for a flow graph of the computations.

Consider the generation of the segment lengths required by the noise footprint program. For the case being considered, we have $\dot{\psi} = 0$ and $\dot{\gamma} \neq 0$ at the junction between straight-line segments. This situation is depicted in figure 4. Since the equations for this case will be similar to those developed earlier for the lateral case, the distance variables have been italicized to distinguish them from those shown in figure 2. The junction points Z_p and Z_q are given by

$$Z_p = Z_\alpha + s_i \mathit{l}_i = Z_\beta - (d_i - s_i)\mathit{l}_i \tag{46}$$

$$Z_q = Z_\beta + c_\beta \mathit{l}_k \tag{47}$$

where s_i and c_β are the quantities to be determined. The center of the circular arc Z_c is given in terms of Z_p and Z_q by

$$Z_c = Z_p + \rho \mathit{l}_p \tag{48}$$

$$Z_c = Z_q + \rho \mathit{l}_q \tag{49}$$

where ρ is the radius of the circular arc, and l_p and l_q are the direction cosines of the two radii shown in figure 4. Equating equations (48) and (49) and utilizing equations (46) and (47) we obtain

$$B\begin{pmatrix} s_i \\ c_\beta \end{pmatrix} = E \tag{50}$$

where

$$B = (\mathit{l}_i - \mathit{l}_k)$$

$$E = d_i \mathit{l}_i + \rho(\mathit{l}_q - \mathit{l}_p)$$

Of the various quantities involved here, l_i and l_k are still given by equation (25), l_p and l_q are given by equations (40) and (41), and d_i is given by

$$d_i = \frac{d_i}{\cos \gamma_i} = \frac{d_i}{\zeta_i} \tag{51}$$

where d_i is defined in equation (2). The remaining variable, the radius ρ, must be based solely on the normal equations since there is now no lateral motion for this case. For a given choice of normal acceleration, a_γ, ρ on the jth segment is given by

$$\rho = \frac{V_j^2}{a_\gamma} \tag{52}$$

The solution of equation (50) is

$$\begin{pmatrix} s_i \\ c_\beta \end{pmatrix} = B^{-1}E \tag{53}$$

and these are the quantities that are needed in order to determine the segment lengths required by the footprint program. The lengths of the ith and kth straight-line segments are then given by

$$m_i = s_i - c_\alpha \tag{54}$$

$$m_k = s_k - c_\beta \tag{55}$$

and they are determined sequentially in conjunction with equation (53) much as has been described earlier in connection with equations (12) and (13). Since the footprint program requires segments in the horizontal plane, the ith and kth segments to be used in the footprint program are given by

$$m_i = m_i \cos \gamma_i = m_i \zeta_i \tag{56}$$

$$m_k = m_k \cos \gamma_k = m_k \zeta_k \tag{57}$$

The equations simplify on the last segment where the γ's on consecutive segments are the same. Thus if the segment after the kth segment has the same inclination angle, it is clear from figure 2 that equation (53) is simply

$$\begin{pmatrix} s_k \\ c_\gamma \end{pmatrix} = \begin{pmatrix} d_k \\ 0 \end{pmatrix}$$

Then equation (55) becomes

$$m_k = d_k - c_\beta$$

and equation (57) becomes

$$m_k = (d_k - c_\beta)\cos \gamma_k$$

$$= d_k - c_\beta \cos \gamma_k \tag{58}$$

Here the d_k is known from equation (2), and the c_β has already been determined. The length of the jth segment is, by observation of figure 4,

$$m_j = c_\beta(\cos \gamma_i + \cos \gamma_k)$$

$$= c_\beta(\zeta_i + \zeta_k) \tag{59}$$

This completes the determination of the segment lengths m_i, m_j, and m_k required by the noise footprint program.

The inclination angles γ_i, γ_j, and γ_k for the ith, jth, and kth segments are also required by the noise footprint program. The values for γ_i and γ_k are known because they were chosen, and the value of γ_j varies continuously between these values. Since a constant value is required by the noise footprint program, a suitable value which gives the correct end point Z_q is

$$\tan \gamma_j = \frac{c_\beta(\sin \gamma_i + \sin \gamma_k)}{m_j} = \frac{\eta_i + \eta_k}{\zeta_i + \zeta_k} \tag{60}$$

This equation can be shown to reduce to the result

$$\gamma_j = \frac{\gamma_i + \gamma_k}{2} \tag{61}$$

The remaining variable needed from the guidance generator is the radius R which for this case with $\dot{\psi} = 0$ is

$$R \equiv 0$$

This condition can be sensed as indicated in figure 1 by determining if consecutive direction cosines, ℓ_i and ℓ_k, are the same (or within some small value ε). Thus,

$$|\ell_i - \ell_k| < \varepsilon \Rightarrow R = 0 \tag{62}$$

Another variable, useful for later purposes, is the angle θ which is given by

$$\cos \theta = \ell_p{}^T \ell_q \tag{63}$$

From equation (63) it can be shown, as expected, that

$$\theta = \gamma_k - \gamma_i \tag{64}$$

Case 4. Longitudinal Acceleration Only (Type C Trajectory: Longitudinal Acceleration with Fixed End Points)

Case 4 typifies the Type-C trajectory in which the path is a straight line in space with longitudinal acceleration between fixed end points. The fixed end points are a result of specifying the points on a land-use map of the terminal area between which the longitudinal acceleration is to occur. A sketch of the situation is shown in figure 5, where d_j is the segment on which the acceleration occurs. A flow graph of the computations is shown in figure 1.

Of the variables to be provided to the footprint program, the segment lengths, d_i, d_j, and d_k are given by equation (2). The variable γ_j is constant at the chosen value, and since there is no lateral motion, $R = 0$. This latter condition can be sensed by equation (62).

The acceleration between the fixed end points needs to be determined to ensure its reasonableness and to enable curved transition trajectories to be determined for other cases. For purposes here, we will estimate the acceleration by determining the constant value of acceleration required to meet the boundary conditions, that is, the initial and final velocities, and the distance traversed. Analysis shows that a point mass moving in a straight line between two points separated by a distance Δ starting with velocity V_i and ending with velocity V_k requires a constant value of acceleration given by

$$a_V = \frac{V_k^2 - V_i^2}{2\Delta} \tag{65}$$

To apply this to the present case, we need only to note from figure 5 that $\Delta = d_j/\cos\gamma$. Thus,

$$a_V = \frac{(V_k^2 - V_i^2)\cos\gamma}{2\,d_j} \tag{66}$$

Case 5. Lateral and Longitudinal Accelerations

In Case 5, the lateral motion is considered first and the longitudinal motion is "fit" within the allowable space. Thus, it is a combination of a Type-A trajectory for the lateral motion and a Type-C trajectory for the longitudinal motion. The lateral equations are generally the same as for the lateral equations developed in Case 1. However, the equation for determining the turn radius will be modified as shown below. The longitudinal equations are the same as developed in Case 4. A flow graph clarifying the computations is shown in figure 1.

The lateral turn radius is based on the total acceleration consisting of the lateral and longitudinal components and is given by

$$a_o^2 = a_\psi^2 + a_V^2$$

$$= \left[\frac{(V_j \cos \gamma)^2}{R}\right]^2 + \left[\frac{(V_k^2 - V_i^2)}{2\Delta}\right]^2 \tag{67}$$

where we have used equations (17) and (65). In this case the distance Δ can be expressed in terms of the lateral turn radius R by

$$\Delta = \frac{R\theta_j}{\cos \gamma} \tag{68}$$

Using the above relationship, we can then solve equation (67) for the lateral turn radius. In addition, since the velocity varies from V_i to V_j, it will be desirable to ensure that the desired value of total acceleration a_o is not exceeded. Further, the sign of R is given by equation (44). Combining these ideas, one obtains

$$R = \text{sgn}[(\alpha_i)(y - y_\gamma)] \max_{n=i,k} \frac{1}{a_o} \left\{(V_n \cos \gamma)^4 + \left[\frac{(V_k^2 - V_i^2)\cos \gamma}{2\theta_j}\right]^2\right\}^{1/2} \tag{69}$$

Case 6. Normal and Longitudinal Accelerations

Case 6 is similar to Case 5 except that the lateral motion is replaced by the normal motion. Thus this case is also a combination of a Type-A trajectory for the normal motion and a Type-C trajectory for the longitudinal motion. The normal equations are obtained from Case 3, but the equations for the radius must be modified as shown below. The longitudinal equations are the same as developed in Case 4. A flow graph of the computations required for this case are summarized in figure 1.

The radius ρ in this case is determined from the total acceleration

$$a_o^2 = a_\gamma^2 + a_V^2$$

$$= \left(\frac{V_j^2}{\rho}\right)^2 + \left(\frac{V_k^2 - V_i^2}{2\Delta}\right)^2 \tag{70}$$

where we have used equations (52) and (65). Now the distance Δ is

$$\Delta = \rho\theta \tag{71}$$

Combining the latter two equations and solving for ρ, we obtain

$$\rho = \max_{n=i,k} \frac{1}{a_o} \left[V_n^4 + \left(\frac{V_k^2 - V_i^2}{2\theta} \right)^2 \right]^{1/2} \tag{72}$$

Case 7. Lateral, Normal, and Longitudinal Acceleration

Case 7 combines the motion due to accelerations in all three axes. Thus it is a combination of Types A, B, and C trajectories. The lateral and normal equations are generally the same as for Case 1. However, the turn radius will be modified as shown below to account for all the components of acceleration. The longitudinal equations come from Case 4 as indicated below. The flow graph of the computations for this case is shown in figure 1.

The turn radius R is determined from the total acceleration which is

$$a_o^2 = a_\psi^2 + a_\gamma^2 + a_V^2 \tag{73}$$

The first component is given in terms of R by equation (17) and the second component is given by equation (34). The third component is given by equation (65). However, it is difficult to determine the distance Δ in that equation because of the combined motions. We will be conservative and take the distance traversed due to lateral acceleration. Thus the distance Δ is given by equation (68) where the γ is now γ_j from equation (35). That is,

$$\Delta = \frac{R\theta_j}{\cos \gamma_j} \tag{74}$$

Hence we have

$$a_o^2 = \left[\frac{(V_j \cos \gamma_j)^2}{R} \right]^2 + \left[\frac{V_j^2 (\zeta_p - \zeta_q)}{R\theta_j} \right]^2 + \left[\frac{(V_k - V_i)^2 \cos \gamma_j}{2R\theta_j} \right]^2$$

To suitably limit a_o it is necessary to know where the maximum occurs on the jth segment. If V_j and $\cos \gamma_j$ are greatest at the same end of the jth segment, the maximum acceleration will occur at that point. If V_j and $\cos \gamma_j$ are not maximum at the same end of the jth segment, the maximum acceleration may theoretically occur anywhere on the segment, and it is difficult to determine where. However, the maximum will nearly always occur where V_j is largest since changes in $\cos \gamma_j$ are inherently very small. Thus we will base the turning on the acceleration at either end of the jth segment. Further, the sign convention of equation (44) will be required. Thus we have

$$R = \operatorname{sgn}[(\alpha_i)(y - y_\gamma)] \max_{n=i,k} \frac{1}{a_o} \left\{ (V_n \cos \gamma_n)^4 + \left[\frac{V_n^2(\zeta_p - \zeta_q)}{\theta_j} \right]^2 + \left[\frac{(V_k^2 - V_i^2)\cos \gamma_n}{2\theta_j} \right]^2 \right\}^{1/2} \tag{75}$$

AIRCRAFT CONTROL GENERATOR

The generation of the optimal aircraft controls is the subject of this section. Given the guidance information, it is desired to have the aircraft follow the commanded trajectory by making the proper choice of the available controls. One of these controls, the engine parameter information, will be required by the noise footprint program. The solution will depend on the class of aircraft to be considered, that is, whether the thrust vector is rotatable and whether the thrust affects the aerodynamic forces.

The aircraft equations of motion will be needed as a starting point for determining the controls. An examination of the equations of motion in various coordinate systems shows the velocity coordinate system to be the most appropriate. A set of orthogonal coordinates is chosen to be in the direction of the velocity vector, perpendicular to the velocity vector in a vertical plane, and perpendicular to the velocity vector in a horizontal plane. A diagram which displays the various forces involved is shown in figure 6. The point-mass dynamic equations are

$$m\dot{V} = T \cos(\alpha + \eta) - mg \sin \gamma - D \tag{76}$$

$$mV\dot{\gamma} = [L + T \sin(\alpha + \eta)]\cos \phi - mg \cos \gamma \tag{77}$$

$$mV\dot{\psi} \cos \gamma = [L + T \sin(\alpha + \eta)]\sin \phi \tag{78}$$

The kinematic equations are

$$\dot{z} = V \sin \gamma \tag{79}$$

$$\dot{x} = V \cos \gamma \cos \psi \tag{80}$$

$$\dot{y} = V \cos \gamma \sin \psi \tag{81}$$

The aerodynamic forces are given in general by

$$D(V,\alpha,T,\delta_F) = \frac{1}{2} \rho V^2 S C_D(\alpha,T,\delta_F) \tag{82}$$

$$L(V,\alpha,T,\delta_F) = \frac{1}{2} \rho V^2 S C_L(\alpha,T,\delta_F) \tag{83}$$

where the inclusion of T represents the effect of thrust on the aerodynamic forces. These equations of motion have three state variables, V, γ, and ψ, and four control variables, T, η, ϕ, and α which are to be determined. It is worth noting that the equations in this coordinate system seem to represent a good balance in simplicity between the dynamic and kinematic equations. For example, if the dynamic equations are written in an earth-fixed coordinate system, the kinematic equations become simpler but the dynamic equations are made more complicated, and a solution for the optimal controls is difficult to obtain.

Now consider the solution of the equations of motion for the controls. Equations (76) to (78) become, when slightly rearranged,

$$T \cos(\alpha + \eta) = mg \sin \gamma + D + m\dot{V} \tag{84}$$

$$L + T \sin(\alpha + \eta) = \frac{mg \cos \gamma + mV\dot{\gamma}}{\cos \phi} \tag{85}$$

$$L + T \sin(\alpha + \eta) = \frac{mV\dot{\psi} \cos \gamma}{\sin \phi} = \frac{m(V \cos \gamma)^2}{R \sin \phi} \tag{86}$$

where in the latter the following basic relationship for the lateral acceleration a_ψ has been used:

$$a_\psi = V\dot{\psi} \cos \gamma = \frac{(V \cos \gamma)^2}{R} \tag{87}$$

The control for ϕ can be obtained uniquely by equating equations (85) and (86):

$$\phi = \tan^{-1} \frac{V\dot{\psi} \cos \gamma}{g \cos \gamma + V\dot{\gamma}} = \tan^{-1} \frac{(V \cos \gamma)^2}{R(g \cos \gamma + V\dot{\gamma})} \tag{88}$$

The controls T and α can be related by solving equations (84) and (85), and the result is

$$T^2 = (mg \sin \gamma + D + m\dot{V})^2 + \left(\frac{mg \cos \gamma + mV\dot{\gamma}}{\cos \phi} - L\right)^2 \tag{89}$$

The two controls η and α can be related by means of equation (84)

$$\eta = \cos^{-1}\left(\frac{mg \sin \gamma + D + m\dot{V}}{T}\right) - L \tag{90}$$

These three equations comprise the relationships to be satisfied for the four controls.

It is now necessary to examine the conditions under which T is constant since the footprint program will accept only constant values. Sufficient conditions are

$$\left.\begin{aligned} \dot{\gamma} = \dot{V} = 0 \\ \text{and} \quad \dot{\psi} = \text{constant} \end{aligned}\right\} \tag{91}$$

Thus, the control equations are

$$\phi = \tan^{-1} \frac{V\dot{\psi}}{g} = \tan^{-1} \frac{V^2 \cos \gamma}{Rg} \tag{92}$$

$$T^2 = [mg \sin \gamma + D(V,\alpha,T,\delta_F)]^2 + \left[\frac{mg \cos \gamma}{\cos \phi} - L(V,\alpha,T,\delta_F)\right]^2 \tag{93}$$

$$\eta = \cos^{-1}\left(\frac{mg \sin \gamma + D}{T}\right) - \alpha \tag{94}$$

If the engine parameter T is not constant, it is approximated here by a linear variation between the two constant values of the preceding and following segments. The footprint program contains this capability. Let T_i and T_k be the constant value of the engine parameter on the ith and kth segments and let T_j be the non-constant value of the engine parameter on the jth segment. Then if one sets $T_j = T_k$ the footprint program will cause T_j to vary with the distance σ as

$$T_j(\sigma) = T_i + (T_k - T_i)\theta(\sigma)$$

where

$$\theta(\sigma) = \frac{\sigma}{304.8} \qquad 0 \leq \sigma \leq 304.8$$

This function causes T_j to vary linearly from T_i to T_k in a fixed distance of 304.8 m (1000 ft). A better procedure would be to vary T_j over the actual computed distance between the ith and kth points. This could be done from equations given earlier, but would require modification to the footprint program.

If the conditions for constant engine parameter T are met, it will be necessary to solve equations (92) to (94). The solution of these equations depends on the class of aircraft to be considered and there are several possibilities. The thrust vector angle η may or may not be rotatable and the thrust vector may or may not affect the aerodynamic forces involved. Thus in the following sections, we will discuss three classes of aircraft.

Class A Aircraft: Thrust Angle Fixed

The Class A aircraft is typified by the CTOL aircraft in which the control η, the angle of thrust vector, is fixed with respect to the aircraft. For simplicity, η is taken to be zero. An aircraft of this class typical of the current fleet is described in reference 3. Further, the aerodynamic forces, lift, and drag are not affected by the engine thrust so that they are

characterized by $D(V,\alpha)$ and $L(V,\alpha)$ for a fixed flap setting. Thus the control equations (92) to (94) become

$$\phi = \tan^{-1} \frac{V\dot{\psi}}{g} = \tan^{-1} \frac{V^2 \cos \gamma}{Rg} \tag{95}$$

$$T^2 = [mg \sin \gamma + D(V,\alpha)]^2 + \left[\frac{mg \cos \gamma}{\cos \phi} - L(V,\alpha)\right]^2 \tag{96}$$

$$T = \frac{mg \sin \gamma + D(V,\alpha)}{\cos \alpha} \tag{97}$$

The first equation gives ϕ based on information from the guidance generator. The second and third each express a relationship between the two controls T and α, so that there is a unique solution. We will not deal with various esoteric approaches for solving these equations. Here we will simply solve the latter two equations simultaneously by a one-dimensional search over α such that equations (96) and (97) are equal. This procedure will be illustrated by a later example.

Class B Aircraft: Thrust Angle Variable

For the Class B aircraft the angle of the thrust vector is rotatable, thus providing another degree of control. In this case equations (92) to (94) form a redundant set of the form

$$\phi = f_\phi(\text{states}) \tag{98}$$

$$T^2 = f_T(\alpha,T,\phi,\text{states}) \tag{99}$$

$$\eta = f_\eta(\alpha,T,\text{states}) \tag{100}$$

These equations contain four control functions, ϕ, T, α, and η and three states, V, γ, and ψ. The redundancy is clear because T and η are uniquely determined from equations (99) and (100) for any arbitrary α. To remove this redundancy requires an additional condition. We will require the additional condition that the noise be minimized by minimizing the engine thrust T. For this reason, interest centers on either equation (93) or (99) in order to satisfy the additional condition. The other control equations are not involved with this additional condition because the determination of the control ϕ from equation (92) or (98) is independent of the other control variables, and the determination of η from equation (94) or (100) follows directly from the solution for the controls T and α. Thus, the additional condition to be imposed is

$$\min_{\alpha} T: \quad T^2 = f_T(\alpha,T,\phi,\text{states}) \tag{101}$$

subject, of course, to any particular constraints on α and η, depending on the type of vehicle. How this equation is solved depends on the aerodynamic

characteristics of the aircraft, that is, whether the aerodynamic forces are affected by the engine parameter, either unavoidably or purposely. Thus, there are two principal types to be considered and two distinctly different approaches for a solution.

Class B1 aircraft: aerodynamics independent of engine parameter- For certain classes of V/STOL aircraft, the aerodynamic forces, lift, and drag, are not affected by the engine parameter T. These Class B1 aircraft have been widely used in various studies such as that of reference 4. Some lift-fan aircraft are in this category and many design studies have been made for these aircraft (refs. 5 and 6). The lift and drag for such vehicles are functions of only two variables; that is, $D(V,\alpha)$ and $L(V,\alpha)$. The consequence of this is that the minimization in equation (101) becomes of the simpler form

$$\min_{\alpha} T: \quad T^2 = f_T(\alpha,\phi,\text{states}) \tag{102}$$

If the aerodynamic forces are given in tabular form, the minimization in equation (102) can be solved by a simple one-dimensional numerical search over α.

If the aerodynamic forces can be approximated by a simple expression, the minimization can be accomplished analytically. The well-known Kuhn-Tucker problem is to

$$\text{Max } f(\alpha)$$

subject to

$$\alpha \leq \alpha_L$$

where α_L is the maximum permitted value of α. Since we want to minimize T, we set $f(\alpha) = -T^2$ where T^2 is given by equation (93). The approximations to be used for lift and drag are

$$D(V,\alpha) = \frac{1}{2}\rho SV^2 C_D = \frac{1}{2}\rho SV^2(D_0 + D_1\alpha^2) \tag{103}$$

$$L(V,\alpha) = \frac{1}{2}\rho SV^2 C_L = \frac{1}{2}\rho SV^2(L_0 + L_1\alpha) \tag{104}$$

Using these approximations, we obtain

$$\left.\begin{aligned} f(\alpha) = -T^2 &= -\left[mg \sin\gamma + \frac{1}{2}\rho SV^2(D_0 + D_1\alpha^2)\right]^2 \\ &\quad -\left[\frac{mg\cos\gamma}{\cos\phi} - \frac{1}{2}\rho SV^2(L_0 + L_1\alpha)\right]^2 \\ &\equiv -(a + b\alpha^2)^2 - (c - d\alpha)^2 \end{aligned}\right\} \tag{105}$$

where a, b, c, and d are functions of γ, V, and ϕ; the functions are apparent from the above equation. The inequality constraint can be made into an equality constraint by the slack variable y:

$$\alpha + y^2 - \alpha_L = 0 \tag{106}$$

Thus, the Lagrangian for this problem is

$$L = -(a + b\alpha^2)^2 - (c - d\alpha)^2 - \lambda(\alpha + y^2 - \alpha_L) \tag{107}$$

and the necessary conditions for a minimum are

$$L_\alpha = -4b^2\alpha^3 - 2(2ab + d^2)\alpha + 2cd - \lambda = 0 \tag{108}$$

$$L_y = -2\lambda y = 0 \tag{109}$$

$$L_\lambda = -(\alpha + y^2 - \alpha_L) = 0 \tag{110}$$

From equation (109) it is seen that there are two possible candidates for the optimum. Either $\lambda = 0$ or $y = 0$, and it is necessary to examine both possibilities to see which will lead to the solution. If $\lambda = 0$, then α is not on the boundary and the optimum α is obtained from the solution of the cubic equation in α, equation (108) with $\lambda = 0$. On the other hand, if $y = 0$, the optimum α is on the boundary. In either case the solution for α can be used to determine T from equation (105) or (93) and the thrust angle η by equation (94). A later example will illustrate this discussion.

Class B2 aircraft: aerodynamics dependent on engine parameter- For many V/STOL aircraft the effect of the thrust parameter on the aerodynamic forces cannot be neglected. Thus the lift and drag are functions of three variables: $L(V,\alpha,T)$ and $D(V,\alpha,T)$. There are many examples of Class B2 aircraft, such as the externally blown flap, the augmentor wing, and the upper surface blowing jet flap aircraft (refs. 7-10).

For this class of aircraft, the thrusting force is a function of a control variable θ, such as throttle setting

$$T = f_T(\theta)$$

and the aerodynamic lift and drag coefficients are functions of two variables for a fixed flap setting:

$$C_L = f_L(\alpha,\theta)$$

$$C_D = f_D(\alpha,\theta)$$

Generally, C_L and C_D will be expressed in graphic form. The variable θ in f_L and f_D reflects the interaction of thrust with the aerodynamics, whether it is unavoidably introduced or whether it is purposely introduced. The consequence of this interaction is that the minimization in equation (101) is

difficult because T appears on both sides of the equation and because C_L and C_D contained in f_T will generally be in graphic form.

The minimization in equation (101) can be solved by a two-dimensional search for the optimal values of T and α. Although various sophisticated approaches for solving equation (101) could be utilized, here we will simply do the following. First, define ε^2 to be the square of the error by which equation (99) or (93) is not satisfied, that is,

$$\varepsilon^2 = T^2 - [mg \sin \gamma + D(V,T,\alpha)]^2 - \left[\frac{mg \cos \gamma}{\cos \phi} - L(V,T,\alpha)\right]^2 \qquad (111)$$

Second, examine the mapping $T\alpha \rightarrow \varepsilon$ by flooding the $T\alpha$ space. Third, select the set $\{T\alpha: \varepsilon = 0\}$, that is, the set satisfying the equations of motion. And fourth, carry out the minimization indicated in equation (101) by selecting the member for which T is minimum. More concisely,

$$\min_{\alpha}\{T: \quad T \in (T,\alpha) \ni \varepsilon = 0\}$$

If desired, the whole process can be carried out directly on the computer so that results of intermediate steps are not displayed.

EXAMPLES

In this section we will illustrate the results of applying the preceding method to the evaluation of noise impact at a typical airport. Figure 7 shows an actual airport, including the airport boundary, the runway, and the surrounding zoning pattern as indicated by the codes. Each of the irregular-shaped areas (even with the same zoning) corresponds to a different land value, with the higher priced land indicated by planned residential zoning generally lying in the southern portion of the map. The noise impact is determined by superimposing a noise footprint on the zoning pattern and by evaluating the total value of land subjected to unacceptable noise levels. For this purpose we will consider the generation of the takeoff footprints for the various types of aircraft. The same equations are valid for landings.

First, we will consider an application to an aircraft of Class A, a representative current CTOL aircraft. For this aircraft class the thrust angle is fixed and the aerodynamic forces are functions of only velocity and angle of attack for a fixed flap position. The data needed here for such an aircraft were taken from reference 3 and are as follows:

$$W = 781{,}047 \text{ N } (175{,}595 \text{ lb})$$
$$S = 144.93 \text{ m}^2 \ (1560 \text{ ft}^2)$$
$$C_L = 0.60 + 0.1065\,\alpha$$
$$C_D = 0.0845 + 1.136\times10^{-4}\,\alpha^2$$
$$T_{max} = 192{,}154 \text{ N } (43{,}200 \text{ lb})$$

The noise source characteristics, which are needed as stored information in the footprint program, consist of data depicting EPNdB as a function of two

variables, the slant range to the observer and the magnitude of the engine parameter (i.e., thrust level). Representative data for current CTOL aircraft are shown in figure 8.

A facsimile of the scope display of the airport and surrounding zoning patterns is illustrated in figure 9. Shown here is the coordinate system starting at the origin of the runway. Also shown on this figure is the flight path passing through the chosen way-points (indicated by small circles) with chosen inclination angles. The way-points are put in directly on the scope display by the operator and sensed by the computer, while the inclination angles are put in on a keyboard. With this information the guidance generator calculations are made in accordance with the equations for Case 3 and the flow diagram of figure 1. The computations made by the guidance generator are sent directly to the footprint program and are not normally made available to the operator. However, for purposes of illustration, these calculations are shown in columns 2, 3, and 4 of the following:

Segment	Guidance generator output				Control generator output		
	Length, m	(ft)	γ, deg	R, m (ft)	T, %	ϕ, deg	α, deg
1	1,524.0	(5,000)	0	0	100	0	0
2	954.87	(3,132.8)	3.75	0	Varies Set to 82.6	0	--
3	30,004.61	(98,440.3)	7.50	0	82.6	0	5.55

The aircraft control generator calculations are determined by the solution of equations (95) through (97). The solution of equations (96) and (97) involves a one-dimensional search for the value of α which satisfies both equations. This is illustrated in figure 10 for the third segment, the only one needed for this simple trajectory. Here the variation of equations (96) and (97) with α is shown, and it can be seen that there are two solutions close together. The desired solution is the one indicated because it requires less thrust and hence results in less noise. The controls for the three segments are summarized in the last three columns of the above table.

The information sent to the footprint program consists of columns 2, 3, 4,and 5 of the above table. The output of the footprint program is given by the single-event noise contour in figure 9. It is seen that the noise impact on the surrounding community is substantial. Moreover, the limited maneuverability of this aircraft relative to the later V/STOL aircraft means that little can be done to alleviate this effect. For example, the ground-track corresponding to a 0.1-g turn starting at an altitude of 304.8 m (1000 ft) is shown by the dotted line in figure 9; the corresponding contour is not shown but it is clear that the noise impact would still be substantial because of the limited maneuverability of this aircraft.

The second example is for Class B1 aircraft which are typified by rotatable thrust vectors and aerodynamic forces that are independent of thrust. A vehicle that fits this category approximately is the lift-fan 100-passenger commercial short-haul transport studied in references 5 and 6. To avoid

repetition, we will illustrate for this example only the aircraft control equations. For this purpose we will take the flight path of the aircraft and the guidance equations to be the same as for the next example, since the aircraft for both examples are highly maneuverable and can readily follow the required path. This path (shown in fig. 11) has been chosen as a potential candidate for minimizing the noise effect on takeoff because it largely avoids much of the residential property. It might be noted that this path does not require the present lift-fan aircraft to utilize its full capability since the path is a STOL flight path whereas the lift-fan aircraft has vertical flight capability.

The aircraft control generator utilizes the output of the guidance generator (see results given in the next example) and the basic aircraft data to determine the optimal control functions. The aircraft characteristics needed for the simplified model here are taken from references 5 and 6 and are

$$\begin{aligned} W &= 561{,}782 \text{ N } (126{,}300 \text{ lb}) \\ S &= 73.21 \text{ m}^2 \text{ } (788 \text{ ft}^2) \\ C_L &= 0.94 + 0.1017\,\alpha \\ C_D &= 0.18 + 0.001342\,\alpha^2 \\ T_{max} &= 646{,}050 \text{ N } (145{,}245 \text{ lb}) \\ \alpha_L &= 10^\circ \end{aligned}$$

where the expressions for C_L and C_D have been fit to aerodynamic data in the above references. The permissible magnitude of the angle of attack α_L is influenced by several considerations. First, vertical gust considerations require that an α safety margin be provided to insure that the peak of the lift curve not be exceeded. Reference 11 indicates the magnitude of this safety margin should be $\sin^{-1}(20/V)^\circ$. Second, the angle of attack should be limited for reasons of passenger comfort, that is, to restrict the pitch attitude of the aircraft. A reasonable limit on α to satisfy both considerations will be taken to be $\alpha_L = 10^\circ$. The solution of the control equations is required for each segment of the flight and follows previous discussion. For segment 3, for example, the control $\phi = 0$. The determination of the control α involves satisfying the necessary conditions given by equations (108) through (110). For this purpose the Lagrangian is

$$L = -(23{,}202.92 + 17.576\,\alpha^2)^2 - (112{,}256.93 - 1{,}331.939\,\alpha)^2 - \lambda(\alpha + y^2 - \alpha_L)$$

Now if $\lambda = 0$, $L_y = 0$ is satisfied. Then

$$L_\alpha = 1235.64\,\alpha^3 + 5.17938\times10^6\,\alpha - 2.99039\times10^8 + \lambda = 0$$

is satisfied by $\alpha = 41.13^\circ$. But then $L_\lambda = -(\alpha + y^2 - 10) = 0$ cannot be satisfied. On the other hand, if $y = 0$, $L_y = 0$ is satisfied, and $L_\lambda = 0$ is satisfied by α on the boundary, that is, $\alpha = \alpha_L = 10^\circ$. Finally, $L_\alpha = 0$ is satisfied for $\lambda = 2.460\times10^8$. Thus, all three necessary conditions for the optimum are satisfied with α on the boundary. The other controls T and η are then found using this value of α and equations (93) and (94). The results for all the controls are summarized for all segments in the following:

CONTROL GENERATOR OUTPUT

Segment	ϕ, deg	α, deg	T, %	η, deg
1	0	0	100	--
2	--	--	Varies Set to 70.3	--
3	0	10	70.3	65.8
4	--	--	Varies Set to 61.7	--
5, 7, 9, 11	0	10	61.7	57.97
6, 8, 10	14.2	10	64.6	59.0

The third application is to a vehicle of class B2 which is characterized by a rotatable thrust vector and aerodynamic forces that are significantly affected by thrust. In accordance with previous discussion, the characteristics of such vehicles are represented in sketch (d) where θ is the primary engine parameter controlling thrust. From an input-output viewpoint, the internal structure is unimportant. However, in order to generate and interpret the input-output characteristics, it is necessary to become concerned with the internal structure for a particular aircraft. It will be convenient for this purpose to use a research version of the augmentor wing aircraft because of the ready availability of the required data.

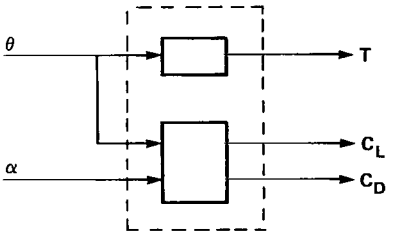

Sketch (d)

The augmentor wing aircraft is provided with direct lift by means of the hot exhaust of the engines which can be rotated downward from horizontal, covering a range of η from 0 to 98°. In addition, the normal lift of the wings has been augmented by the addition of a cold air duct and flap redesign that exhausts the cold air along the wing. This results in added lift due to increased circulation. For such a vehicle the internal structure is as shown in sketch (e), where θ is the engine throttle angle, T is the thrust due to the hot exhaust gas, T_C is the cold thrust, and C_J is the cold thrust coefficient defined by $C_J = T_C/qS$. The characteristics of the unlabeled boxes were obtained from reference 9 and are shown in figures 12 and 13.

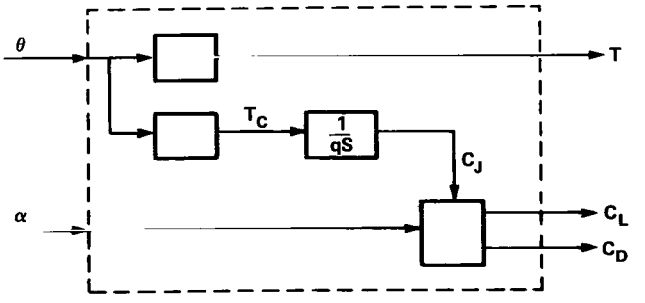

Sketch (e)

It is worth reiterating that the aerodynamic characteristics shown are representative of this class of aircraft in which thrust interacts with aerodynamic forces. That is, the lift and drag coefficients are

invariably given as a function of two variables, the angle of attack and an interaction parameter (such as C_J) related to the thrust (see data given in ref. 7 for a variety of configurations). Although the physical mechanism of this interaction depends on the specific aircraft type, the input-output characteristics are all described by similar kinds of data.

The remaining characteristics of the vehicle under study are (see ref. 9):

$$W = 177{,}920 \text{ N } (40{,}000 \text{ lb})$$
$$S = 80.36 \text{ m}^2 \ (865 \text{ ft}^2)$$
$$T_{max} = 61{,}605 \text{ N } (13{,}850 \text{ lb})$$

Finally, the noise characteristics may vary depending on the aircraft type and the level of noise suppression technology incorporated into the aircraft. Since the sensitivity of noise effect to the level of noise suppression is of inherent interest, we will take the two different levels, A and B (fig. 14) to illustrate the results. Level B is taken from unpublished FAA data which are approximately the same as data given in reference 7, while level A has been increased by 10 dB in order to investigate the sensitivity to this parameter.

The flight path chosen for the aircraft to fly is shown by the facsimile of the scope display in figure 11. The way-points, which are chosen directly on the scope display, are indicated by the small circles, and the inclination angles, which are put in through the keyboard, are also indicated. With this information, the guidance generator calculations are made in accordance with previous discussion. Again, the results of these computations are normally sent directly to the footprint program and are not available for inspection. However, the results are illustrated in the following.

GUIDANCE GENERATOR OUTPUT

Segment	γ, deg	R, m (ft)	V, knots	Length or angle, m (ft) or deg
1	0	0	Varies	194.9 (639.4)
2	4.75	0	70	218.2 (715.8)
3	9.5	0	70	196.5 (644.6)
4	9.5	0	Varies	914.4 (3,000)
5	9.5	0	100	239.6 (786.2)
6	9.5	+1050.71 (+3447.2)	100	38.8°
7	9.5	0	100	254.3 (834.2)
8	9.5	+1050.71 (+3447.2)	100	27.4°
9	9.5	0	100	847.2 (2,779.4)
10	9.5	+1050.71 (+3447.2)	100	45.8°
11	9.5	0	100	6037.4 (19,807.8)

The information in columns 2, 3, and 5 are sent to the footprint program while the information in columns 2, 3, and 4 are sent to the aircraft control program.

The generation of the optimal controls follows the theory previously described. The mapping $T_{x\alpha} \rightarrow \varepsilon$ has been investigated numerically and the

set obtained for which $\varepsilon = 0$ (see eq. (111)). For illustration, this set is displayed in figure 15 for segment 5 of the flight path. Also shown is the other control η. From this figure, the removal of the redundancy by the minimization in equation (101) so as to minimize the noise amounts to simply choosing the minimum T subject to constraints on α and η. It can be seen that the true minimum T occurs at essentially the boundary of the η constraint $\eta \leq 0$ as shown. The computer program does not locate this point precisely because of the finite increments in T used (limited to about 80 lb). Thus, the computer program solution is slightly in error. Note that this error results in a significant difference in η between the two points. However, this is an academic point that is not of great concern because the engine parameter T, which determines the noise impact, is essentially the same for either solution. A more sophisticated optimization procedure could locate the true minimum precisely, but this was not considered necessary here. A summary of the results of calculations for all the controls over the entire flight path is shown in the following. Of the controls shown, only the data for T needs to be sent to the footprint program.

CONTROL GENERATOR OUTPUT

Segment	ϕ, deg	α, deg	T, %	η, deg
1	0	0	100	--
2	--	--	Varies Set to 55.3	--
3	0	10.96	55.3	10.55
4	--	--	Varies Set to 59.78	--
5, 7, 9, 11	0	2.51	59.78	9.86
6, 8, 10	14.24	2.95	60.36	8.5

The output of the footprint program is displayed in figure 16 by the single-event 90 EPNdB contours. The two contours represent the results for the two different levels of technology. For the level A technology, it is seen that the noise effect on the residential property is fairly small because of the capability of the aircraft to fly a curved path that avoids most of the noise-sensitive areas. Further, the steep flight-path capability contributes to this reduction. On the other hand, the level B technology is sufficient to confine the noise effect to within the airport boundary. Comparisons such as this are of obvious use in investigating the sensitivity of the actual noise impact to the noise technology level of the aircraft.

CONCLUDING REMARKS

A few points regarding this paper are worth emphasizing. The methodology presented here allows complete flexibility in determining the desired flight path of the aircraft. This is important because advanced V/STOL aircraft have much greater maneuvering capability than the conventional current CTOL

aircraft. If the advantages of this greater maneuverability in terms of increased airspace capacity, reduced delays, reduced noise, etc., are to be shown, the methodology must be flexible enough to be able to account for these greater capabilities. The methodology discussed here is flexible enough to permit the simultaneous consideration of maneuvers in all three axes. Also, the transitions between straight-line segments are uniquely defined, that is, there is no necessity to iterate between the transition flight paths and the accelerations.

There are a number of areas for further research and development. First, since this report was restricted to the development of the equations, further work should deal with the implementation of the computer program of the models to provide the desired on-line interactive capability. Second, further development of the footprint program that was used could be made in the following directions:

1. The speed of the program could be increased for better man-machine interaction.

2. The maximum number of segments allowed could be increased from the present four.

3. A relatively minor change could be made to enhance on-line operation so as to give the operator control of the termination of the contour computations rather than allowing the program itself to terminate the computations, sometimes prematurely.

4. The program could be changed to avoid the possibility of producing an incorrect noise level at a given observer position by basing the computations on the segment producing the greatest noise rather than on the closest segment.

5. The program could be improved to incorporate anisotropic noise characteristics.

Finally, the generation of the aircraft control functions was not dealt with adequately. Sophisticated optimization methods could be utilized to great advantage to seek out the desired solutions more efficiently than was done here.

Ames Research Center
National Aeronautics and Space Administration
Moffett Field, California 94035, November 17, 1977

REFERENCES

1. A Study of the Magnitude of Transportation Noise Generation and Potential Abatement. Serendipity, Inc. for Department of Transportation. DOT-OS-A9-018, November 1970.

2. Safeer, Harvey B.; and Williams, Louis J.: Airport Noise Exposure Contour Model User Manual. Department of Transportation, No. OST-ONA 72-3, August 24, 1972.

3. Snyder, C. Thomas: Analog Study of the Longitudinal Response of a Swept-Wing Transport Airplane to Wind Shear and Sustained Gusts During Landing Approach. NASA TN D-4477, April 1968.

4. Mehra, R. K.; and Bryson, Jr., A. E.: Conjugate Gradient Methods with an Application to V/STOL Flight-Path Optimization. Journal of Aircraft, vol. 6, no. 2, March-April 1969.

5. Addendum to Conceptual Design of V/STOL Lift-Fan Commercial Short-Haul Transports, 1980-1985. Final Report, vol. IV, The Boeing Company, March 5, 1971.

6. Zabinsky, J. M.; Minker, W. F.; Bohn, J. G.; Derbyshire, T.; Middlebrooks, J. E.; Barron, J. P.; Williams, B.; and Miller, C. W.: V/STOL Lift Fan Commercial Short-Haul Transports, NASA CR-2437, prepared by Boeing Commercial Airplane Company, March 1974.

7. Study of Quiet Turbofan STOL Aircraft for Short-Haul Transportation. Final Report, vol. II, Aircraft. NASA CR-114607, prepared by Douglas Aircraft Company, June 1973.

8. Quiet Turbofan STOL Aircraft for Short-Haul Transportation. Final Report, vol. I. NASA CR-114612, prepared by Lockheed Aircraft Corporation, June 14, 1973.

9. Rumsey, P. C.; and Spitzer, R. E.: Simulator Model Specification for the Augmentor Wing Jet STOL Research Aircraft. NASA CR-114434, prepared by The Boeing Company, December 1971.

10. Quigley, H. C.; Innis, R. C.; and Grossmith, S.: A Flight Investigation of the STOL Characteristics of an Augmented Jet Flap STOL Research Aircraft. NASA TM X-62,334, May 1974.

11. Scott, B. C.; Hynes, C. S.; Martin, P. W.; Bryder, R. B.: Progress Toward Development of Civil Airworthiness Criteria for Powered-Lift Aircraft. FAA-RD-76-100 and NASA TM X-73,124, prepared for U.S. Dept. of Transportation, May 1976.

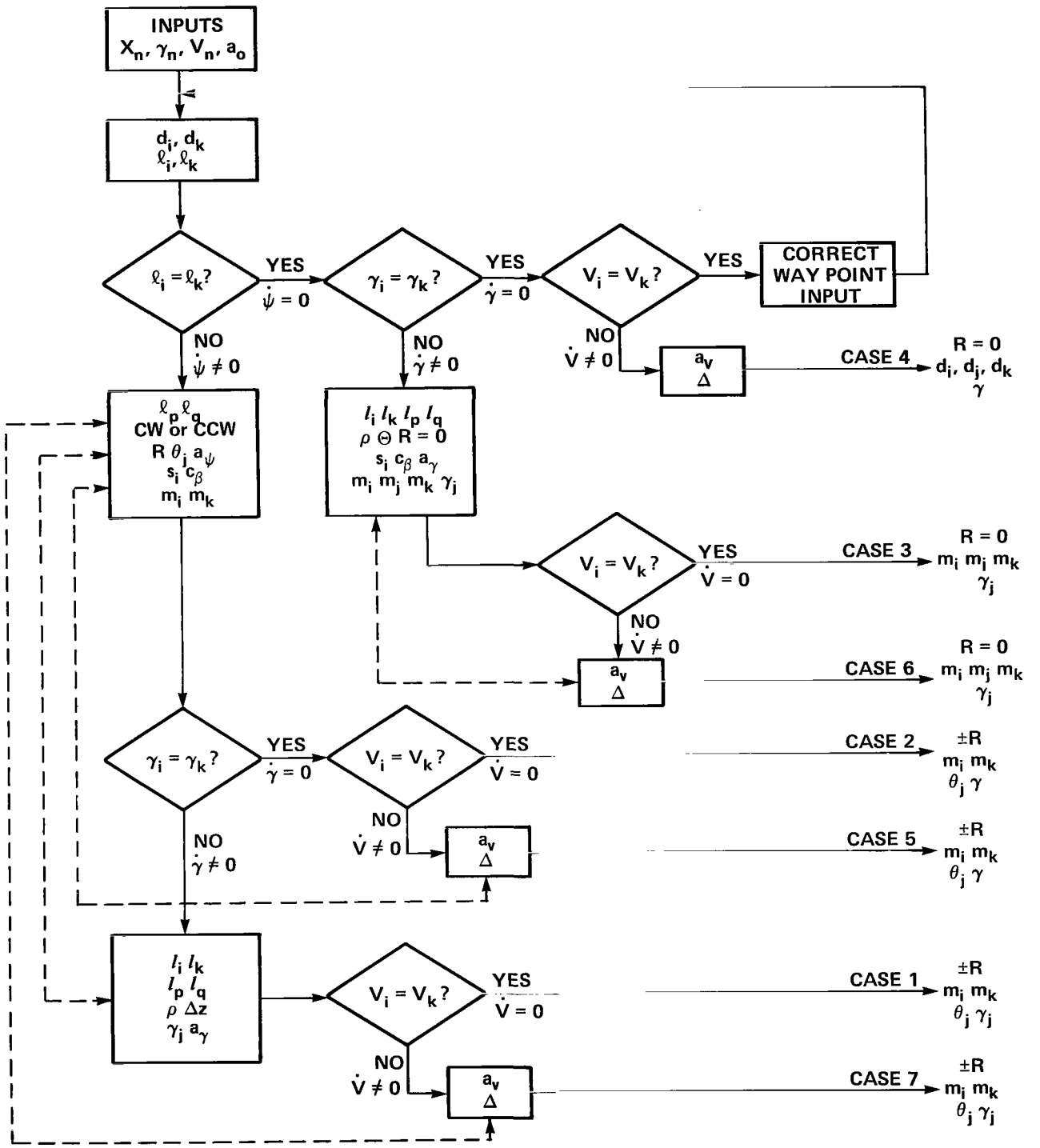

Figure 1.- Flow graph of guidance generator computations.

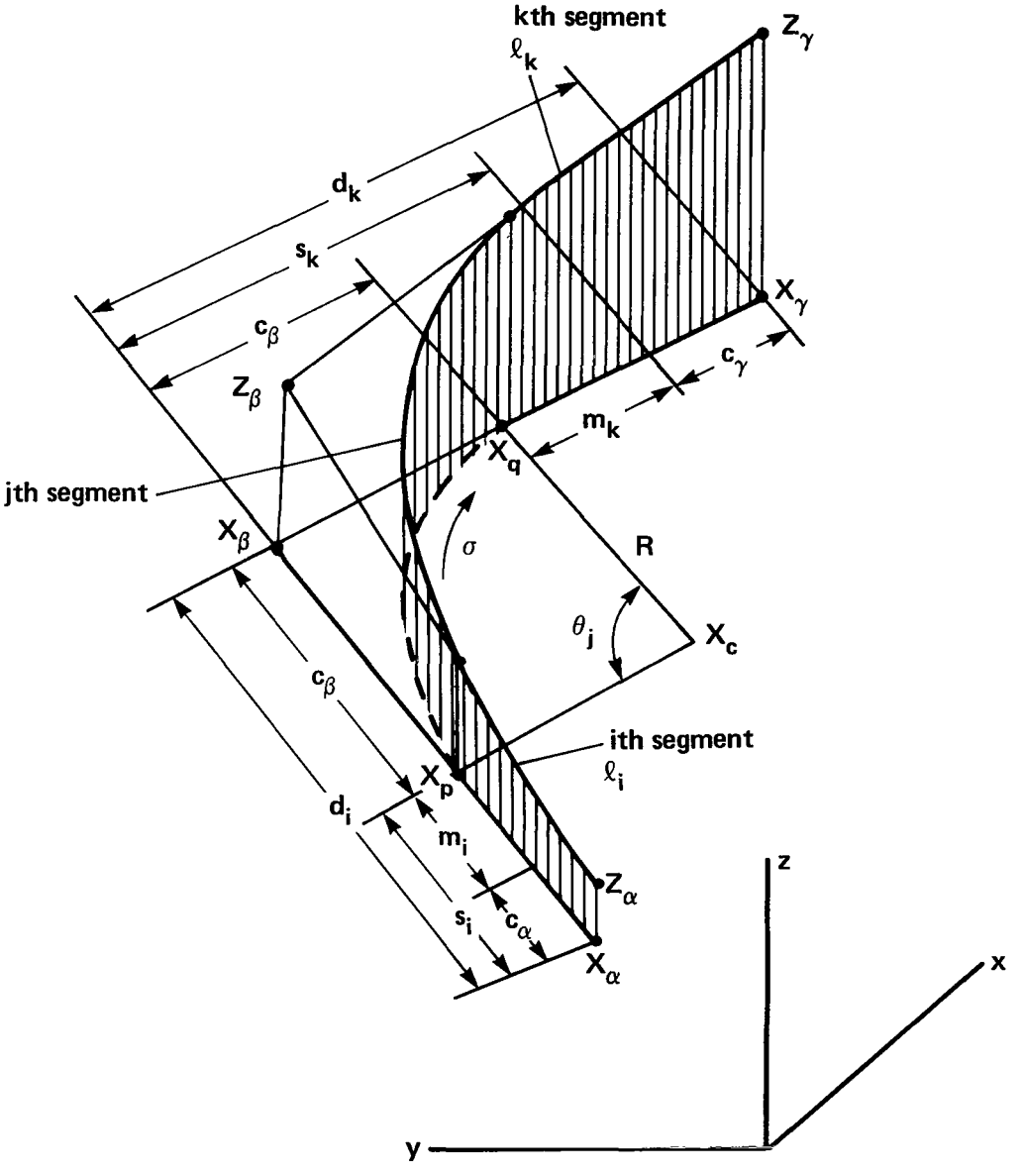

Figure 2.- Illustration for Case 1: Lateral and normal accelerations.

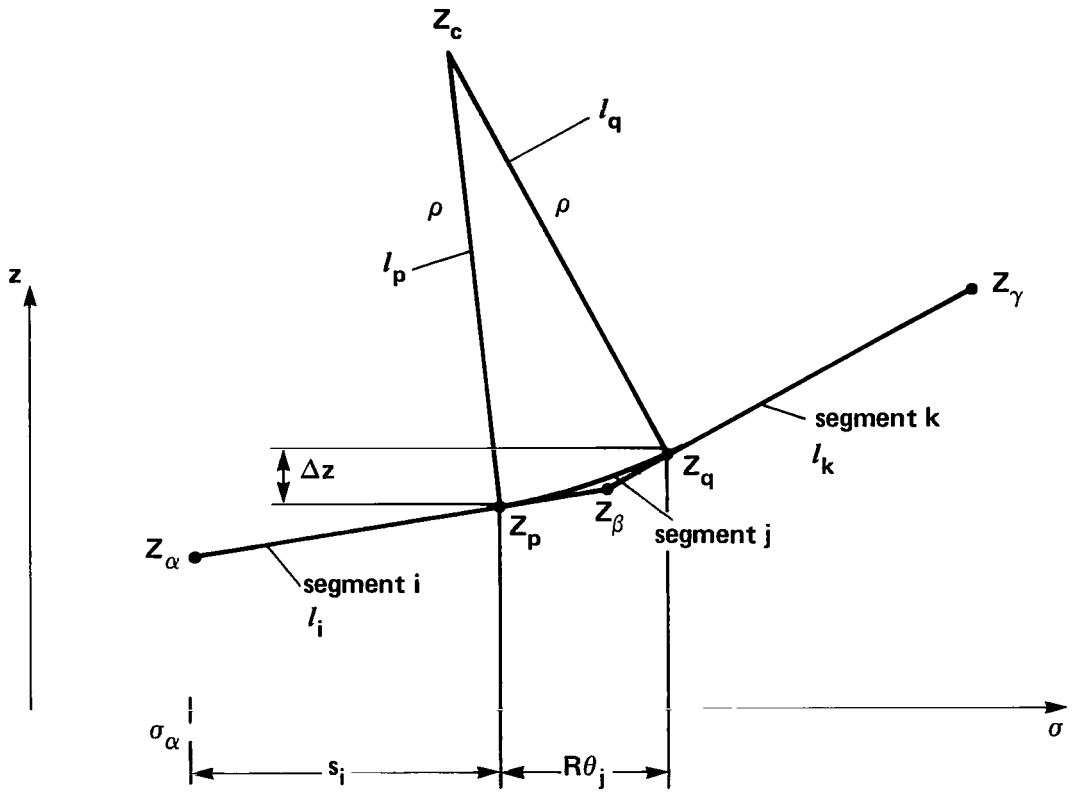

Figure 3.- Illustration for Case 1: Normal trajectory with fixed end points.

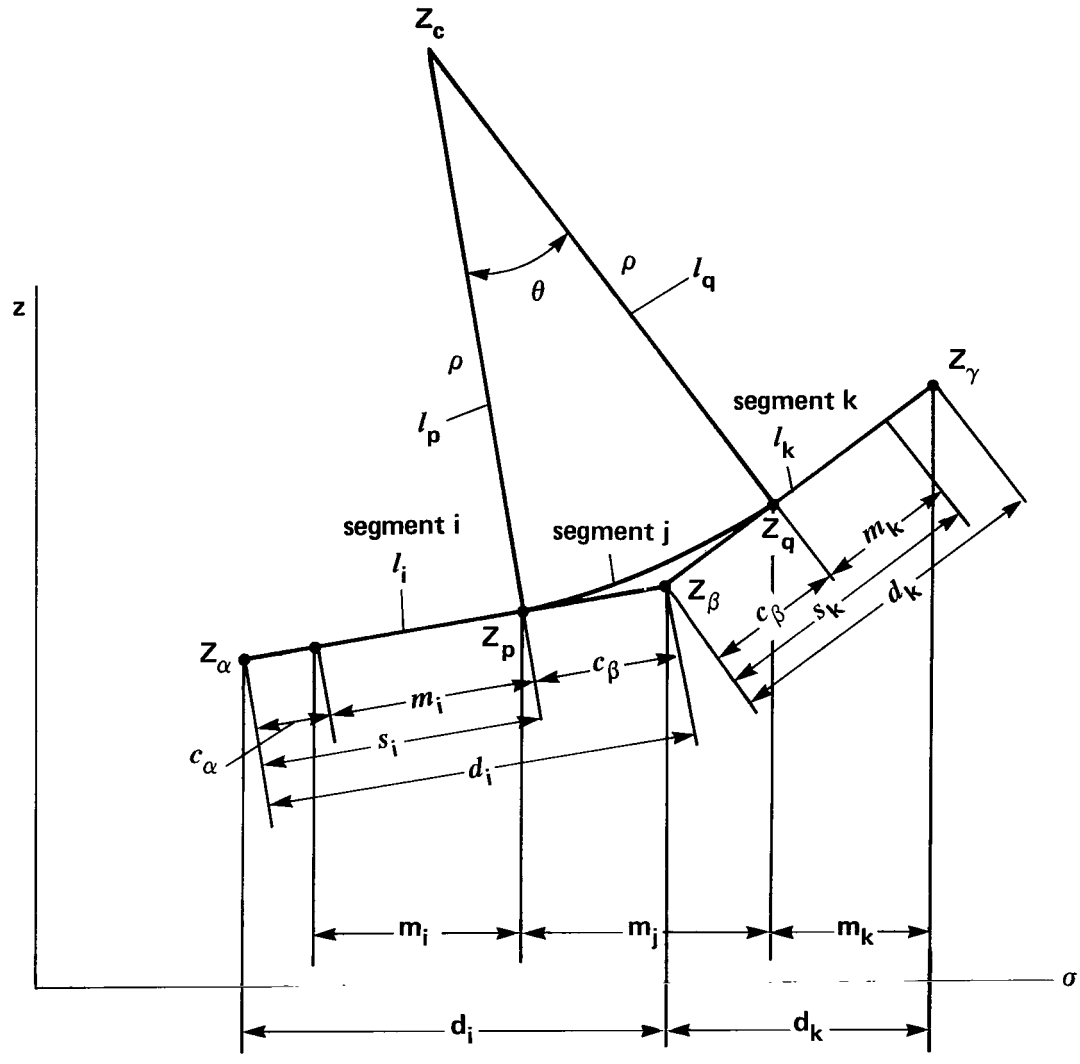

Figure 4.- Illustration for Case 3: Normal acceleration only.

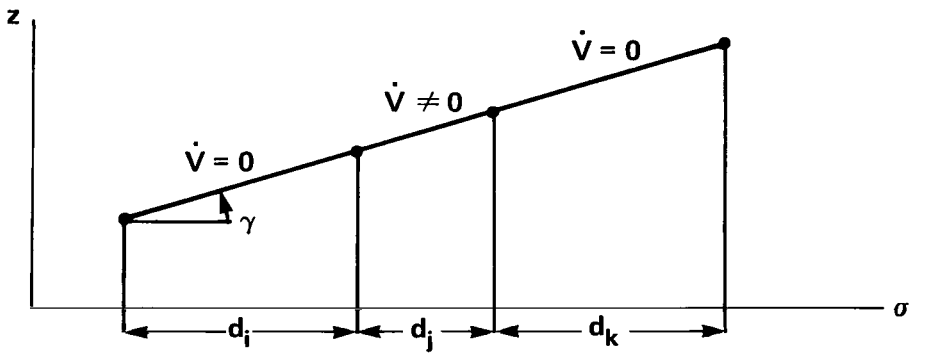

Figure 5.- Illustration for Case 4: Longitudinal acceleration only.

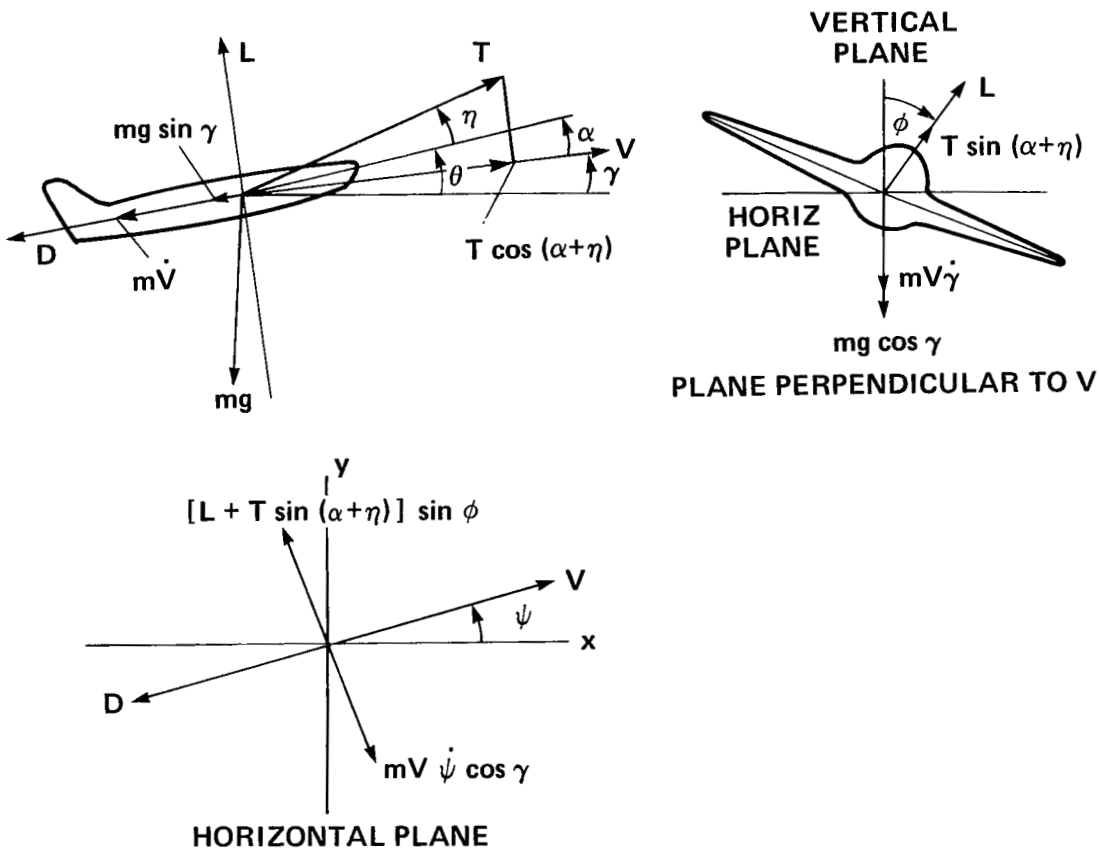

Figure 6.- Diagram of forces.

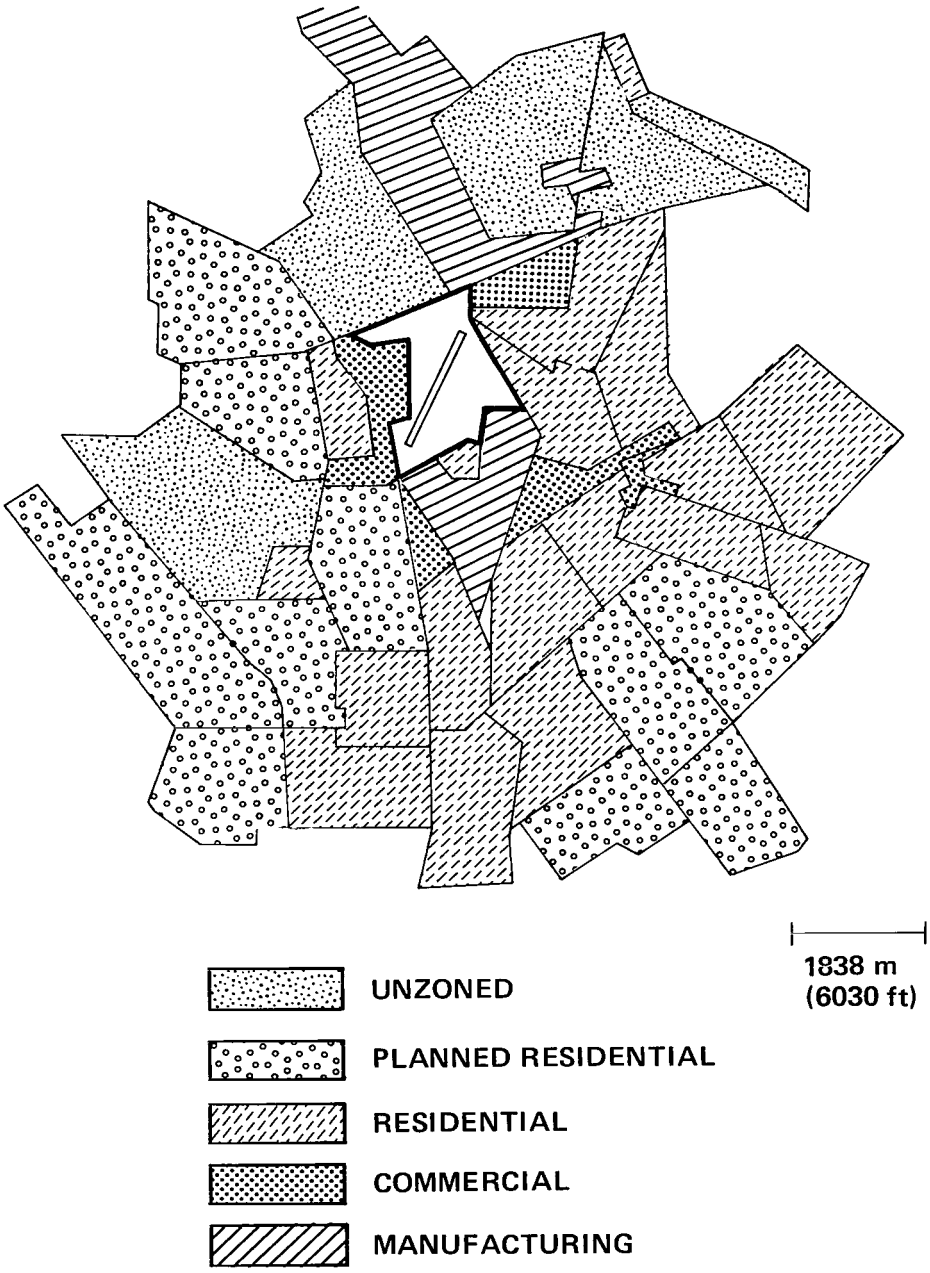

Figure 7.- Typical airport and surrounding community.

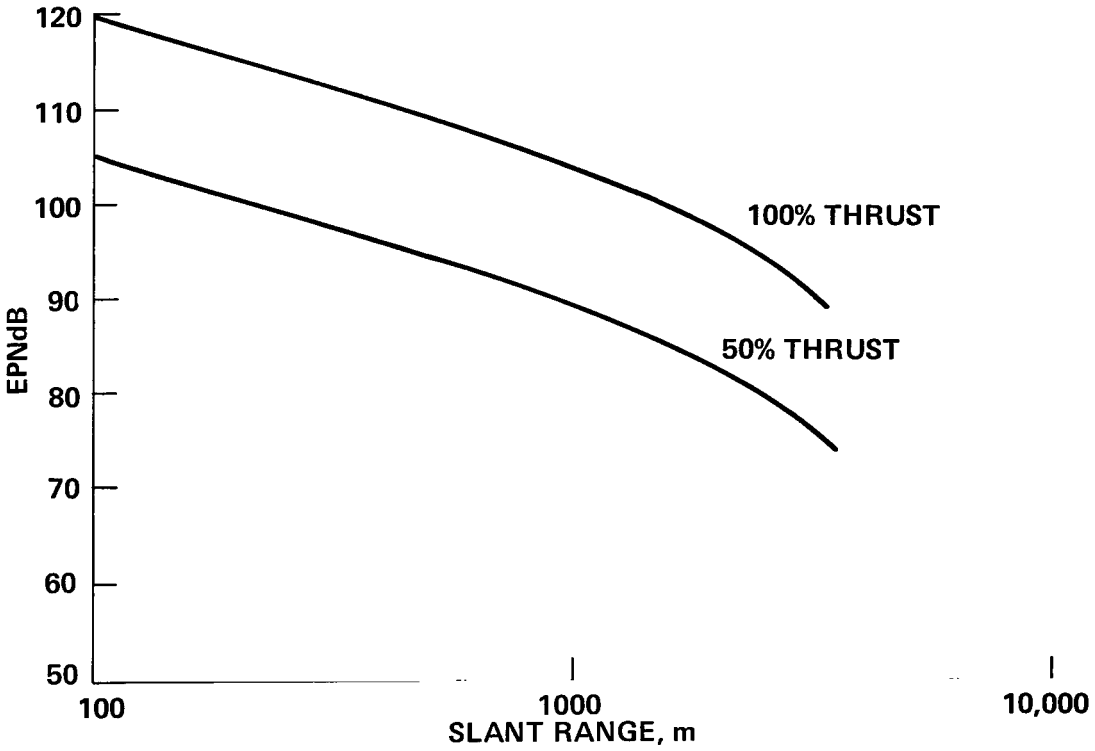

Figure 8.- Noise characteristics for example CTOL aircraft.

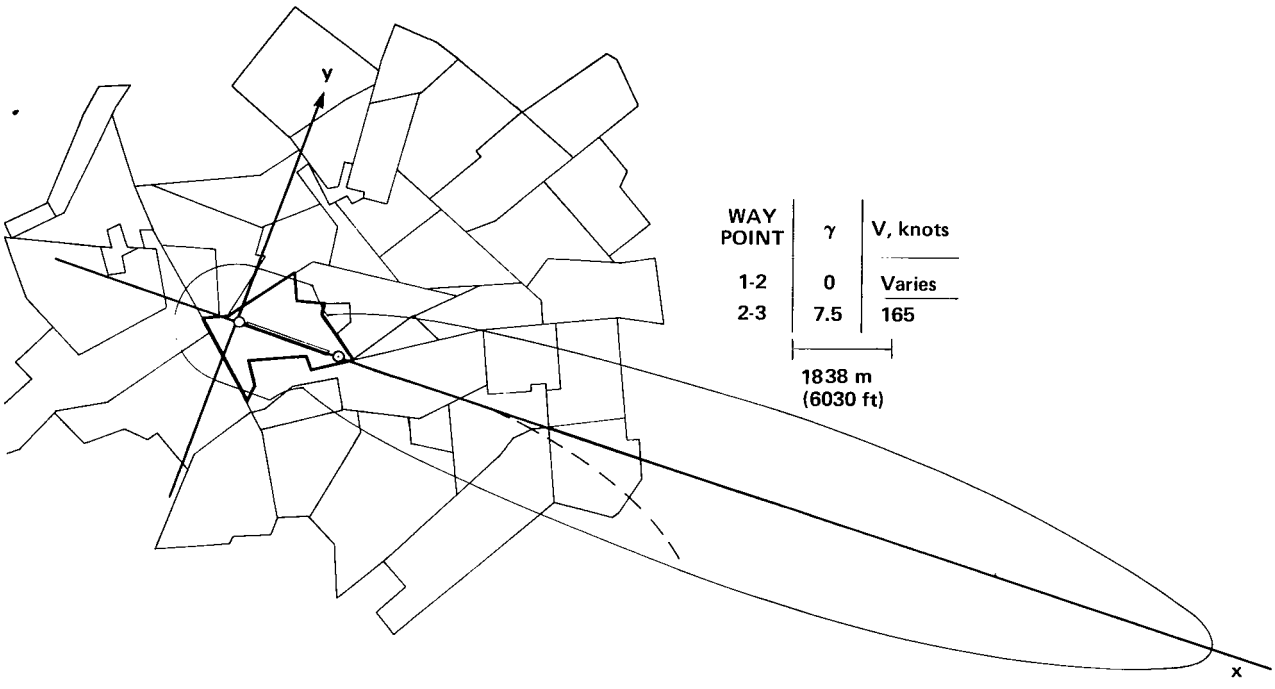

Figure 9.- Flight path and 90 EPNdB noise footprint for example CTOL aircraft.

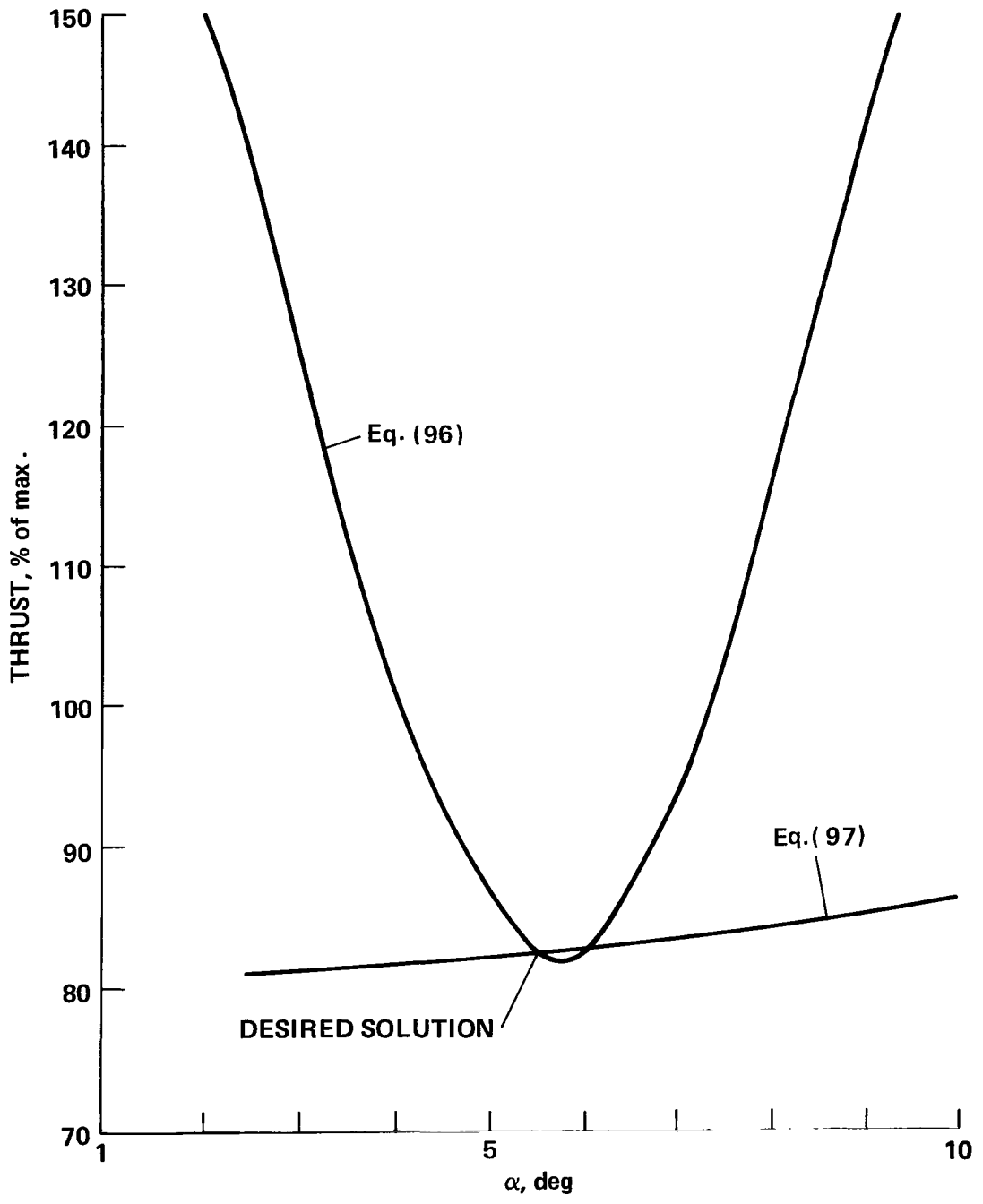

Figure 10.- Solution for controls T and α for example CTOL aircraft.

WAY POINTS	γ, deg	V, knots
1-2	0	Varies
2-3	4.75	70
3-4	9.5	70
4-5	9.5	Varies
5-6	9.5	100
6-7	9.5	100
7-8	9.5	100

Figure 11.- Flight path for example STOL aircraft.

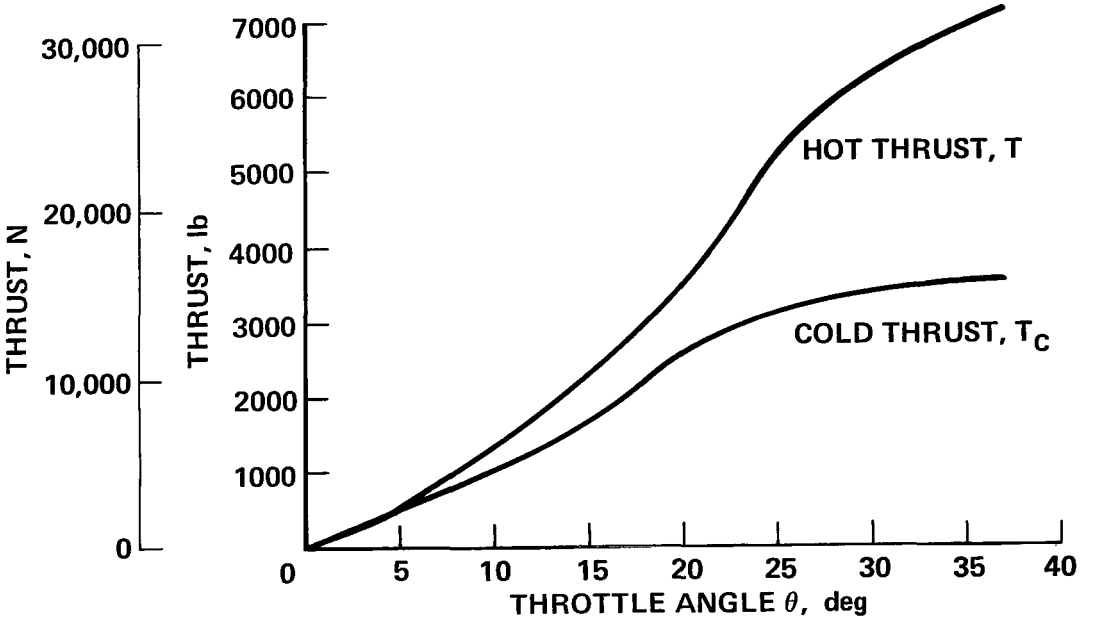

Figure 12.- Hot and cold thrust versus throttle angle for example jet STOL aircraft.

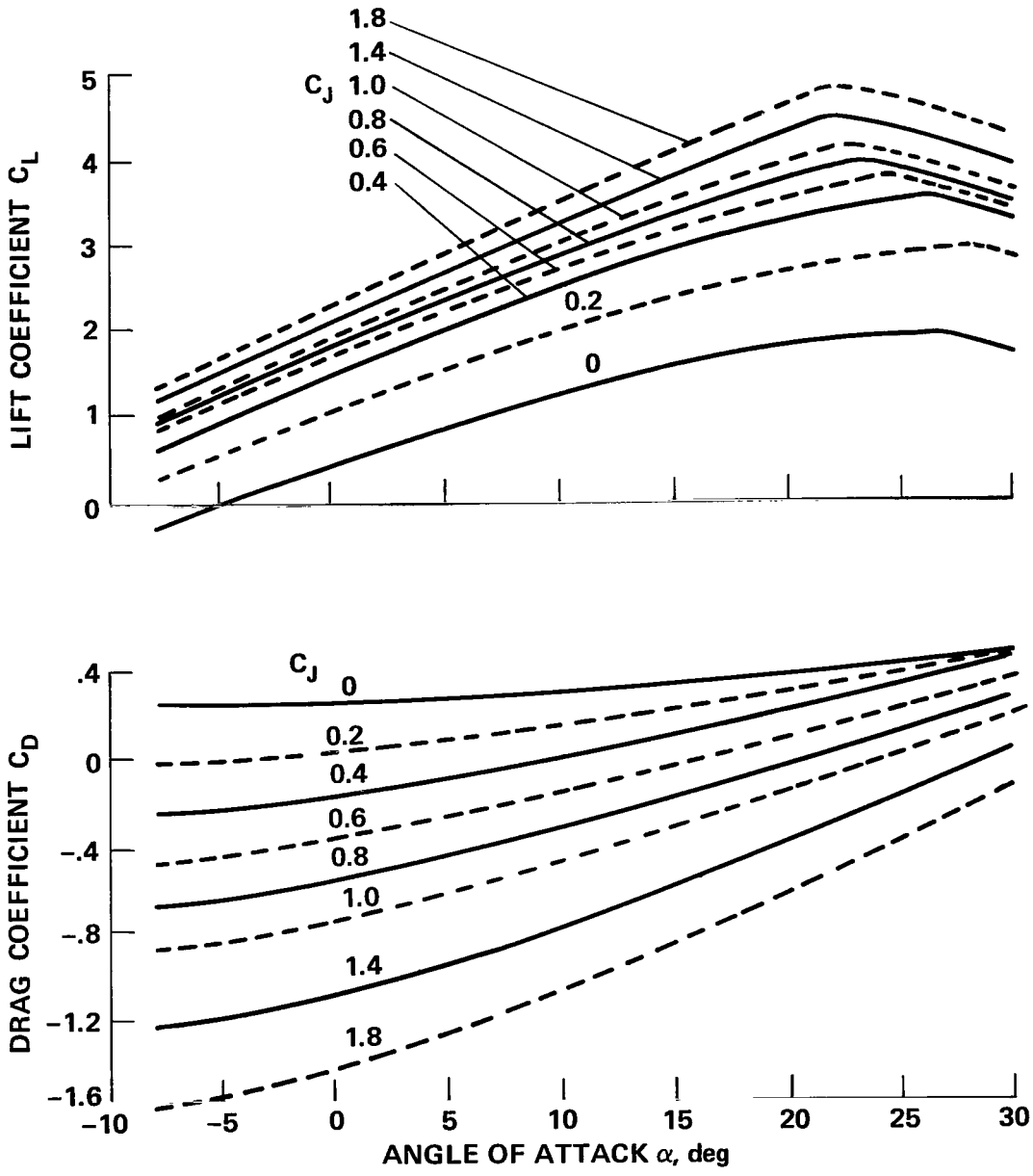

Figure 13.- Lift and drag for example jet STOL aircraft; $\delta_F = 30°$.

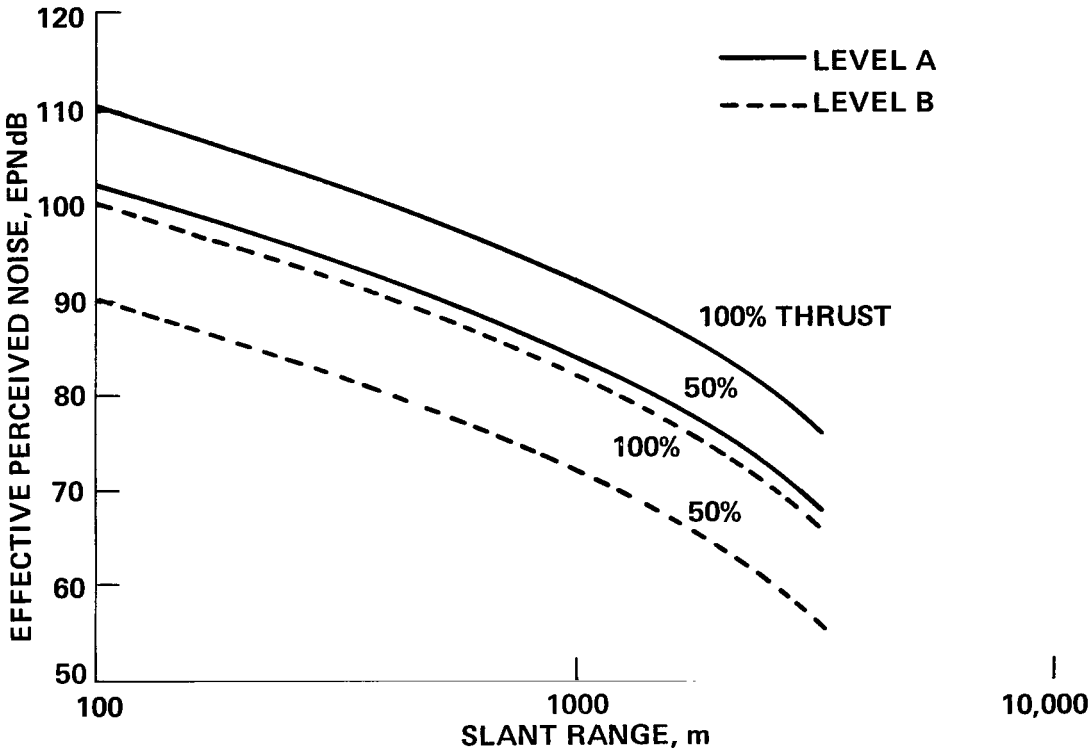

Figure 14.- Noise characteristics for example jet STOL aircraft.

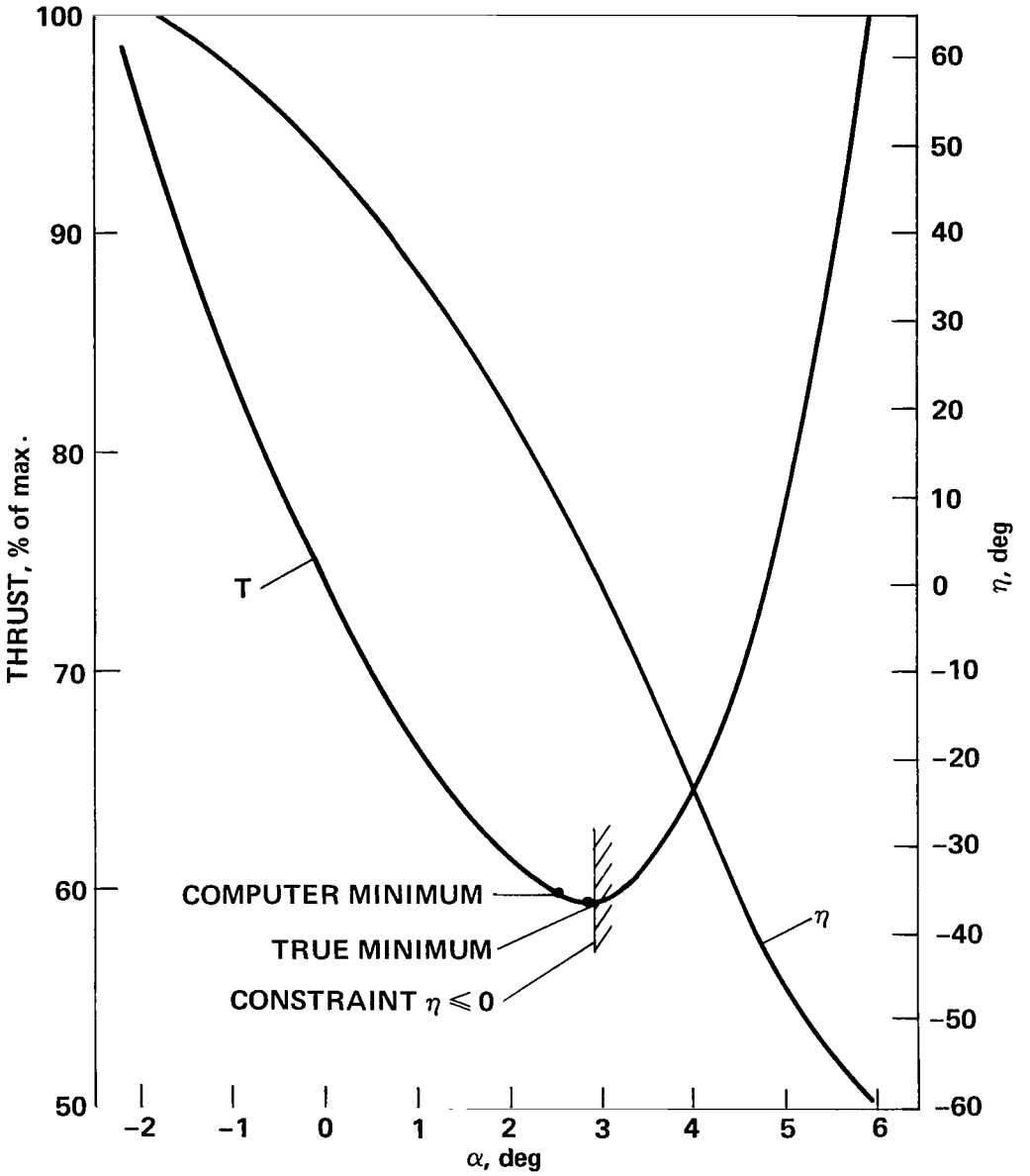

Figure 15.- Optimal controls for example powered-lift STOL aircraft of Class B2; Segment 5.

Figure 16.- 90 EPNdB noise footprints for example STOL aircraft.

1. Report No.	2. Government Accession No.	3. Recipient's Catalog No.
NASA TP 1237		

4. Title and Subtitle	5. Report Date
OPTIMAL GUIDANCE AND CONTROL FOR INVESTIGATING AIRCRAFT NOISE-IMPACT REDUCTION	May 1978
	6. Performing Organization Code

7. Author(s)	8. Performing Organization Report No.
Elwood C. Stewart and Thomas M. Carson	A-7121
	10. Work Unit No.
	513-53-06

9. Performing Organization Name and Address	11. Contract or Grant No.
NASA Ames Research Center Moffett Field, Calif. 94035	
	13. Type of Report and Period Covered
	Technical Paper

12. Sponsoring Agency Name and Address	14. Sponsoring Agency Code
National Aeronautics and Space Administration Washington, D.C. 20546	

15. Supplementary Notes

16. Abstract

As part of a NASA program to investigate technical approaches for increasing the terminal area effectiveness of advanced short-haul aircraft, this report is concerned with a methodology for investigating the reduction of community noise impact. There are a number of computer programs available for the generation of noise footprints, all of which require various input data that are usually unavailable. This report is concerned with the development of two models to provide such data: a guidance generator and an aircraft control generator suitable for various current and advanced types of aircraft. The guidance generator produces the commanded path information from inputs chosen by an operator from a graphic scope display of a land-use map of the terminal area. The guidance generator also produces smoothing at the junctions of straight-line paths. The aircraft control generator determines the optimal set of the available controls such that the aircraft will follow the commanded path. The solutions for the control functions are given and shown to be dependent on the class of aircraft to be considered, that is, whether the thrust vector is rotatable and whether the thrust vector affects the aerodynamic forces. For the class of aircraft possessing a rotatable thrust vector, the solution is redundant; this redundancy is removed by the additional condition that the noise impact be minimized. Information from both the guidance generator and the aircraft control generator is used by the footprint program to construct the noise footprint.

The complete package of models provides a useful methodology for constructing an interactive graphics tool for rapidly assessing the effects of different aircraft technologies, flight paths, aircraft mixes, and other variables, and for the minimization of noise impact. These effects are illustrated, utilizing an existing footprint program, by several examples which consist of three broad classes of CTOL and V/STOL aircraft.

17. Key Words (Suggested by Author(s))	18. Distribution Statement
Noise-impact reduction Aircraft control Aircraft guidance	Unlimited STAR Category - 08

19. Security Classif. (of this report)	20. Security Classif. (of this page)	21. No. of Pages	22. Price*
Unclassified	Unclassified	58	$4.50

*For sale by the National Technical Information Service, Springfield, Virginia 22161

NASA-Langley, 1978